

Disaster Risk through Investors' Eyes: a Yield Curve Analysis*

Joan Margalef[†]

This version: November 15, 2024

[Click here for latest version](#)

Abstract

This paper develops a model to estimate investors' perceived probability of disaster from yield curve data. Disasters are extreme events like defaults or interstate wars with significant economic impact. By integrating an asset pricing model with government bond yields from Datastream, I provide daily estimates of the one-year-ahead disaster probability as perceived by investors for approximately 60 countries from 2000 to 2023. The use of yield curve data offers a high-frequency measure of disaster risk that can rapidly incorporate new information. Several facts indicate that the estimated probabilities have predictive value. Probabilities spike before disaster events, such as the debt restructurings of Greece, Sri Lanka, and Ghana, and the onset of the Russia-Ukraine war. They are also strongly associated with higher-risk credit ratings. In a forecasting exercise using machine learning, the estimated disaster probabilities enhance the predictive power of credit ratings. This demonstrates the informational value of bond market data in predicting events.

Keywords: Disaster Risk, Yield Curve, Asset Pricing

JEL Classification: E20, G01, G12, G15, G17

*Margalef acknowledges the financial support from the FPI grant from the Spanish Ministry of Science Innovation and Universities (PRE2020-093943). All errors are mine.

[†]Universitat Autònoma de Barcelona and Barcelona School of Economics (joan.margalef@bse.eu)

1 Introduction

There are many reasons to care about investors' beliefs about the future. First, these beliefs can be used to predict economic outcomes. Investors have financial incentives to be accurate in their predictions. They synthesize information from diverse sources and embed it into their actions, influencing asset prices. This is the basis of the Efficient Market Hypothesis, which posits that asset prices reflect all available information and adjust quickly to new developments.¹ Second, their beliefs carry significant economic consequences. If investors assign a higher probability of government default, they will demand higher returns, increasing the debt burden and, in turn, making default more likely.² Even if a default does not occur, the increased debt burden raises financial stress, amplifies uncertainty, and might force the government to implement austerity measures.³ For these reasons, authorities seek to manage investors' beliefs through effective communication and policy interventions.⁴ These reasons are especially relevant in the context of economic disasters, such as defaults, interstate wars, or depressions, given their profound economic consequences. Thus, understanding and monitoring investors' perceived probability of disaster can be crucial for anticipating disasters and informing policy actions. The challenge is that investors' beliefs are not directly observable. However, since asset prices are directly influenced by these beliefs,⁵ they can be used to reveal the probability of disaster as perceived by investors.

This paper provides a model to extract investors' perceived probability of disaster from yield curve data. The yield curve, which plots government bond yields against their maturities, consolidates investors' beliefs over different time horizons. It is widely regarded as a crucial financial indicator with proven forecasting power.⁶ By integrating an asset pricing model with yield curve data from Datastream, I provide daily estimates of the one-year-ahead disaster probability as perceived by investors for approximately 60 countries from 2000 to 2023. Then, I study the predictive value of these probabilities through several exercises.

To estimate the disaster probabilities, I use a classic asset pricing model, based on Rietz (1988) and Barro (2006), that incorporates time-varying disaster probabilities. A representative consumer max-

1. This notion originates from Fama (1970). See Malkiel (2003) for a review. Prediction markets exemplify this principle by aggregating beliefs through trading contracts on future events, such as elections or sports outcomes, often demonstrating remarkable predictive accuracy (Wolfers and Zitzewitz 2004; Arrow et al. 2008).

2. Lorenzoni and Werning (2019) show that high interest rates, driven by fears of default, can create self-fulfilling debt crises. De Grauwe and Ji (2013) find that Eurozone government bond markets are susceptible to self-fulfilling liquidity crises.

3. Reinhart and Rogoff (2010) find that countries with debt exceeding 90 percent of GDP experience notably lower median and mean growth rates. In emerging economies, they identify a more sensitive threshold, where external debt exceeding 60 percent of GDP leads to a two percent decline in annual growth.

4. Blinder et al. (2008) highlights that communication has become a crucial tool in monetary policy, significantly influencing financial markets, the predictability of policy decisions, and achieving macroeconomic objectives.

5. Ross (2015) refers to disaster risk as *dark matter*: "It is unseen and not directly observable but exerts a force that can change over time and profoundly influence markets."

6. Substantial empirical evidence suggests that the yield curve is one of the most informative indicators, particularly for forecasting economic downturns (Estrella and Hardouvelis 1991; Estrella and Mishkin 1998; Ang, Piazzesi, and Wei 2006). Even the Federal Reserve Bank of New York has a webpage dedicated to the yield curve and its predictive power for recessions. See https://www.newyorkfed.org/research/capital_markets/ycfaq.html and https://www.newyorkfed.org/medialibrary/media/research/capital_markets/Prob_Rec.pdf. Furthermore, other studies show that the yield curve responds to economic policy uncertainty (Leippold and Matthys 2022), political uncertainty (Pástor and Veronesi 2013; Smales 2016) and international political risk (Huang et al. 2015).

imizes expected consumption in a closed economy where she can invest in government bonds. The equilibrium conditions imply that prices depend on the expectation of consumption growth, inflation, and sovereign default. The occurrence of a disaster induces significant shifts in these variables, which I refer to as “jumps”. Thus, the probability of such disasters shapes investors’ expectations regarding these variables, and then prices. The nature of these “jumps” varies depending on the type of disaster being analyzed: sovereign default or interstate war. The model implies that observed bond prices can be decomposed into a theoretical non-disaster price and a disaster wedge. The non-disaster price reflects the price determined by current business cycle conditions. The theoretical model is general and simple enough to be calibrated to many countries, allowing us to compute the non-disaster theoretical prices for each of them over time. I bring the model to the data by regressing observed bond prices on the computed theoretical non-disaster prices using a fixed effects regression. By exploiting variation across countries, time periods, and maturities, this approach accounts for potential model misspecifications and isolates key fixed effects essential for estimating the disaster wedge. Finally, by specifying a type of disaster based on each country’s context, I estimate the disaster probability.

To assess the predictive value of the estimated disaster probabilities, I first analyze through case studies how they evolve before disasters. This reveals how investors anticipate them and respond to new information as the disaster approaches. Second, I examine their relationship with credit ratings data. Finally, I conduct a series of forecasting exercises using machine learning techniques to evaluate the added value of the estimated disaster probabilities. I assess whether these probabilities enhance the prediction of downgrades, upgrades, and disaster events relative to a model that uses only credit ratings data. Specifically, I compare the Area Under the Curve (AUC) of the Receiver Operating Characteristic (ROC) curve and the Precision-Recall (PR) curve across three models: one using only disaster probabilities, another using only credit rating variables, and a third combining both sources.

Probabilities spike before disaster events, such as the debt restructurings of Greece, Sri Lanka, and Ghana, as well as the onset of the Russia-Ukraine war. In some cases, such as Greece and Ghana, the probabilities reached 100% months before the event, while in others, sharp increases to around 30% were observed weeks in advance, eventually approaching certainty in the days before the disaster. This suggests that investors respond quickly to new information and adjust probabilities as the disaster approaches. Furthermore, disaster probabilities are strongly associated with higher-risk credit ratings. Finally, the estimated probabilities enhance the predictive power of credit ratings for predicting future downgrades and disaster events. For downgrades, adding disaster probabilities to the credit ratings model improves the ROC-AUC from 0.84 to 0.88 and the PR-AUC from 0.15 to 0.26. For disasters, the ROC-AUC increases from 0.94 to 0.97, and the PR-AUC rises from 0.75 to 0.92. However, no significant improvement is observed for upgrades. Overall, these findings demonstrate the informational value of bond market data in predicting events.

The disaster probabilities estimated in this study have numerous potential applications. They can help identify effective policies to shape investor beliefs, measure the welfare effects of these policies,

and examine disaster spillover effects on neighboring countries. The computed disaster probabilities will be available on my GitHub repository⁷, enabling researchers and policymakers to incorporate them into their own analyses.

This article relates to at least two strands of literature. The first is the macroeconomic literature on “(rare) disasters” or “tail events”. The early disaster literature was theoretical, addressing asset pricing puzzles—such as the risk-free rate premium—by introducing the concept of a low-probability of a “consumption” disaster (Rietz 1988; Barro 2006; Gabaix 2008; Backus, Chernov, and Martin 2011; Gourio 2012; Gabaix 2012; Wachter 2013; Farhi and Gabaix 2016).⁸ A consumption disaster unifies extreme events like wars and depressions into a single concept, representing any significant decline in consumption observed in U.S. history. More recently, advancements in econometric techniques and the availability of richer datasets have fueled a new wave of research focused on empirically estimating the probability of these consumption disasters. This body of research is largely based on reduced-form models (Berkman, Jacobsen, and Lee 2011; Schreindorfer 2020). A notable utility-based model in Barro and Liao (2021) uses option prices and fixed-effect regressions to estimate consumption disaster probabilities across major economies.⁹ This paper contributes both methodologically and through its practical applications. First, it introduces a structural model to estimate disaster probabilities from high-frequency yield curve data. The yield curve data I use is particularly insightful due to its panel data structure, including a maturity dimension, and its well-established role as a key financial indicator. The model is flexible enough to be calibrated for a wide range of countries, offering daily updates, and it can account for different types of disasters, not just consumption disasters. This is important because consumption disasters are rare and may not be the most salient risk. The model can be calibrated to capture defaults and wars, which can occur more frequently, especially considering the broad sample of 60 countries. Second, the paper assesses the predictive value of the computed disaster probabilities, paving the way for their use in future applications.

Secondly, financial literature has extensively examined the predictive power of asset prices, including the government yield curve, in forecasting economic outcomes. A widely used measure is the sovereign yield spread, which compares yields from “safe” countries like Germany or the U.S. to those from riskier assets, such as foreign bonds.¹⁰ Yields and their spreads have been frequently applied in reduced-form models, capturing sovereign default and political risks (Clark 1997; Remolona, Scatigna, and Wu 2007; Bekaert et al. 2016), financial crises (Bluwstein et al. 2023),¹¹ and wars (Chadefaux 2017). This paper adds to this body of research by leveraging the yield curve in a structural model.

7. <https://github.com/joanmargalef>

8. Julliard and Ghosh (2012) argue that rare events alone cannot adequately explain asset pricing puzzles like the equity premium.

9. Ross (2015) introduces the Recovery Theorem, a method for disentangling investors’ natural beliefs about future returns and their degree of risk aversion, allowing to recover the probability of a catastrophe.

10. The spread between corporate and government bonds is also commonly used as an indicator of economic activity (Gilchrist and Zakrajšek 2012; Gilchrist et al. 2016), and corporate default risk (Duffee 1999; Dionne et al. 2010). Another method for corporate default risk is the Merton Distance to Default model (Merton 1974; Bharath and Shumway 2008).

11. This model integrates the yield curve into a machine learning framework.

Computing the theoretical non-disaster price that accounts for current business cycle conditions, I “control” for factors unrelated to disasters that also influence yields. This approach addresses the limitation of relying solely on the yield spread, which ignores that countries differ in their business cycle conditions and that not all of the spread is due to default risk. Furthermore, it’s important to differentiate between the predictive power of asset prices and whether the beliefs inferred from these prices are ultimately accurate, a distinction that has only recently begun to receive attention.

This paper is structured as follows. The next section outlines the asset pricing model. In Section 3, I present the methodology for estimating investors’ perceived probability of disaster. In Section 4, I discuss the results, followed by the conclusions in the final section.

2 Model setup

The model follows Rietz (1988) and Barro (2006), which I extend by including time-varying probabilities of disasters. It will later be calibrated separately for 64 countries, but for clarity and simplicity, the country-specific indices are omitted in this section.

The representative consumer maximizes a time-additive utility function:

$$\mathbb{E}_t \sum_{t=0}^{\infty} \beta^t U(C_t), \quad (1)$$

where β is the time discount factor and the period utility function, $U(C_t)$, takes the CRRA form

$$U(C_t) = \frac{C_t^{1-\theta}}{1-\theta} \quad (2)$$

θ is the coefficient of relative risk aversion. In each period, agents can invest in government nominal zero-coupon bonds, each of which will pay out one unit of currency at maturity. Q_{Nt} is the price at t of a bond that matures in N periods, and X_{Nt} is the amount bought. The government can default on its obligations and pay a fraction F_{Nt} of the bond’s face value. F_{Nt} represents the recovery rate. $F_{Nt} = 1$ indicates full payment with no default, and $F_{Nt} = 0.8$ implies that the government pays 80% of the bond’s face value. The budget constraint of the agents is given by

$$P_t C_t = W_t - \sum_{N=1}^H Q_{Nt} X_{Nt} \quad \forall t \quad (3)$$

where P_t is the price of consumption and W_t corresponds to the wealth if no bond is bought, which includes the payments from previously purchased bonds.¹² H represents the maximum maturity. Using

12. The model shows a closed economy, where all that is produced is consumed. The BIS report Fang, Hardy, and Lewis (2022) shows that the majority of government bonds are held by domestic investors, especially during crises.

the usual first-order conditions, I derive the fundamental asset pricing equation:

$$Q_{Nt} = \beta^N \mathbb{E}_t \left[\frac{U'(C_{t+N})P_t}{U'(C_t)P_{t+N}} \right] \quad (4)$$

The relationship between bond prices and bond yields is given by

$$Y_{Nt} = \left(\frac{1}{Q_{Nt}} \right)^{\frac{1}{N}} - 1 \quad (5)$$

where Y_{Nt} is the yield of a bond that matures in N periods at time t . The yield curve is the graph that plots Y_{Nt} against N . This equation allows us to translate bond prices to yields and vice versa.

Substituting in the functional form of the marginal utilities of consumption, Equation 4 can be rewritten as

$$Q_{Nt} = \beta^N \mathbb{E}_t \left[\frac{F_{Nt}}{\prod_{j=1}^N G_{t+j}^\theta \Pi_{t+j}} \right] \quad (6)$$

with $G_{t+1} = C_{t+1}/C_t$ being consumption growth and $\Pi_{t+1} = P_{t+1}/P_t$ being inflation. Note that bond prices decrease in expected consumption growth and inflation. Since the bond is a mechanism to transfer consumption to the future, there are fewer incentives to buy the bond if consumption is expected to be high. Higher expected inflation diminishes the real value of the bond. The price also decreases as the expected recovery rate decreases.

Following the standard approach in asset pricing, I will analyze this equilibrium price equation using exogenous processes for consumption growth, inflation, and the recovery rate.¹³

In each period, a disaster may or may not occur. For simplicity, disasters are assumed to be independent of one another. $\delta_{\tau,t}$ denotes the probability at t of a disaster happening in τ periods s.t.

$$\delta_{\tau+1,t} = \phi_\delta \delta_{\tau,t} \quad (7)$$

with $\phi_\delta \in [0, 1]$ being the persistence parameter of the disaster probability. This allows us to express all disaster probabilities in terms of $\delta_{1,t}$ since $\delta_{\tau,t} = \phi_\delta^{\tau-1} \delta_{1,t}$.

The law of motion of consumption growth is

$$G_{t+1} = \alpha_G G_t^{\phi_G} \varepsilon_{t+1} V_{t+1} \quad (8)$$

where α_G is a constant term, ϕ_G represents a persistence parameter, $\varepsilon_{t+1} \stackrel{\text{iid}}{\sim} \log N(0, \sigma_\varepsilon^2)$ is white noise, and $V_{t+\tau}$ is the “disaster impact factor on consumption growth” s.t.

$$V_{t+\tau} = \begin{cases} 1 & \text{if no disaster at } t + \tau \\ J_G & \text{if disaster at } t + \tau \end{cases} \quad (9)$$

13. See Cochrane (2009).

Therefore, the disaster affects consumption growth through V_{t+1} . When the disaster does not occur, the log of consumption growth follows an AR(1) process. $J_G > 0$ represents the “jump” in consumption growth induced by the disaster. A value of $J_G = 0.98$ implies that the disaster reduces consumption growth by 2%. Note that the disaster directly impacts consumption growth in the same period it occurs and indirectly in future periods. If the disaster occurs at $t + 1$, it will directly impact G_{t+1} through V_{t+1} . Additionally, it will indirectly affect G_{t+2}, G_{t+3}, \dots through their dependence on G_{t+1} .

Analogously, the process of inflation is

$$\Pi_{t+1} = \alpha_{\Pi} \Pi_t^{\phi_{\Pi}} \eta_{t+1} W_{t+1} \quad (10)$$

where α_{Π} is a constant term, ϕ_{Π} is the persistence parameter, $\eta_{t+1} \stackrel{\text{iid}}{\sim} \log N(0, \sigma_{\eta}^2)$ is white noise, and $W_{t+\tau}$ is the “disaster impact factor on inflation” s.t.

$$W_{t+\tau} = \begin{cases} 1 & \text{if no disaster at } t + \tau \\ J_{\Pi} & \text{if disaster at } t + \tau \end{cases} \quad (11)$$

$J_{\Pi} > 0$ represents the “jump” in inflation induced by the disaster. A $J_{\Pi} = 1.05$ means the disaster increases inflation by 5%. As with consumption growth, the disaster directly impacts inflation in the same period it occurs and indirectly in future periods.

When a disaster occurs, there is a probability γ that it will lead to a sovereign default, which I model as an equal haircut across all bonds. When there is no disaster, the probability of default is zero. Then, the recovery rate is given by

$$F_{Nt} = 1 \cdot \prod_{\tau=1}^N Z_{t+\tau} \quad (12)$$

with $Z_{t+\tau}$ being the “disaster impact factor on the recovery rate” s.t.

$$Z_{t+\tau} = \begin{cases} 1 & \text{if no disaster at } t + \tau \\ 1 & \text{if disaster but no partial default at } t + \tau \\ 1 - J_F & \text{if disaster and partial default at } t + \tau \end{cases} \quad (13)$$

$J_F \in [0, 1]$ denotes the size of the haircut. A $J_F = 0.2$ means that the government does not pay 20% of the face value of the bond. A $J_F = 1$ is full default. The product of $Z_{t+\tau}$ over all periods until maturity implies that haircuts are cumulative, making long-term bonds riskier since they can suffer several haircuts.

Note that independence between disasters implies that the disaster impact factors are independent across periods, i.e., $V_t \perp V_{t'}, W_{t'}, Z_{t'} \text{ for } t' \neq t$. However, V_t, W_t , and Z_t are perfectly correlated through the disaster event.

Given this, the bond price from Equation 6 can be expressed as

$$Q_{Nt} = \underbrace{Q_{Nt}^{ND}}_{\text{Non-disaster price}} \underbrace{\prod_{\tau=1}^N (1 + \phi_{\delta}^{\tau-1} \delta_{1,t} (J_{\tau,N} - 1))}_{\text{Disaster wedge}} \quad (14)$$

Q_{Nt}^{ND} represents the bond price in the absence of disasters, and $J_{\tau,N}$ synthesizes all the jump effects of a disaster happening in τ periods to a bond that matures in N periods. I refer to $J_{\tau,N}$ as the “overall jump”. Remember that $\delta_{1,t}$ is the probability at t of a disaster happening in 1 period. Thus, the price of the bond consists of the non-disaster price, Q_{Nt}^{ND} , multiplied by a “disaster wedge” that accounts for the risks of all disasters that may occur before the bond reaches maturity. This wedge depends on the disaster probabilities for all periods before maturity, $\delta_{\tau,t} = \phi_{\delta}^{\tau-1} \delta_{1,t}$ for $\tau \in [1, N]$, and the potential impact of each, summarized in $J_{\tau,N}$. For example, a 2-period bond is affected by the risk of a disaster happening in 1 and 2 periods, but not after, as it will have already matured. The term $1 + \phi_{\delta}^{\tau-1} \delta_{1,t} (J_{\tau,N} - 1)$ is the specific disaster wedge induced by the disaster in τ periods. Long-term bonds accumulate more elements in the product, as they are exposed to more periods where disasters can occur.

The functional form of the non-disaster price is

$$Q_{Nt}^{ND} = \beta^N \frac{e^{\frac{1}{2} (\sum_{i=1}^N (\sum_{j=0}^{i-1} \phi_G^j)^2 \theta^2 \sigma_{\varepsilon}^2 + \sum_{i=1}^N (\sum_{j=0}^{i-1} \phi_{\Pi}^j)^2 \sigma_{\eta}^2)}}{\left(\alpha_G^{\sum_{i=1}^N i \phi_G^{N-i}} G_t^{\sum_{i=1}^N \phi_G^i} \right)^{\theta} \alpha_{\Pi}^{\sum_{i=1}^N i \phi_{\Pi}^{N-i}} \Pi_t^{\sum_{i=1}^N \phi_{\Pi}^i}} \quad (15)$$

This incorporates the expectations based on current business cycle conditions since it contains the effect of current consumption growth (G_t) and inflation (Π_t).

Finally, the functional form of $J_{\tau,N}$ is

$$J_{\tau,N} = \frac{1 - \gamma J_F}{J_G^{\sum_{j=1}^{N+1-\tau} \theta \phi_G^{j-1}} J_{\Pi}^{\sum_{j=1}^{N+1-\tau} \phi_{\Pi}^{j-1}}} \quad (16)$$

This illustrates that the effect of a disaster depends on the interplay between jump effects in consumption growth (J_G), inflation (J_{Π}), and default risk (γ and J_F), which may offset each other. As the gap between the disaster’s occurrence (τ) and bond maturity (N) increases, the summations in the exponents include more components. This reflects that long-term bonds have more indirect effects by a single disaster due to the persistence of the underlying variables’ processes (ϕ_G and ϕ_{Π}). As a result, short- and long-term bonds may behave very differently, even in opposite directions. For example, if a disaster causes a sharp drop in consumption growth and moderate inflation, but consumption growth is less persistent, the recessionary impact will be strong initially, leading to an increase in short-term bond prices. However, as the effect fades quickly and inflation persists, long-term bond prices will eventually decrease as inflation outweighs the recessionary impact.

This model offers tractable solutions for decomposing bond prices and allows us to analyze how

disaster probabilities affect them.

Proposition 1 *The bond price with maturity N at time t , Q_{Nt} , decreases with the probability of a disaster occurring in the next period, $\delta_{1,t}$, if and only if*

$$\sum_{\tau=1}^N \frac{\phi_{\delta}^{\tau-1} (J_{\tau,N} - 1)}{1 + \phi_{\delta}^{\tau-1} (J_{\tau,N} - 1)} < 0 \quad (17)$$

A sufficient condition for this to hold is that $J_{\tau,N} < 1$ for all τ .

The proof is in the appendix. When $\delta_{1,t}$ increases, all $\delta_{\tau,t}$ increase due to its persistence parameter, $\phi_{\delta} \in [0, 1]$. The overall effect is ambiguous because, $J_{\tau,N}$ may be greater than or less than 1 for different values of τ . However, if $J_{\tau,N} < 1$ for all periods τ , then Q_{Nt} will decrease as $\delta_{1,t}$ increases.

3 Estimating investors' perceived probability of disaster

The model, summarized by Equation 14, shows that government bond prices can be decomposed into a non-disaster theoretical price and a disaster wedge. To estimate disaster probabilities, I first calibrate the model for every country to compute theoretical non-disaster prices. Then, I bring the model to the data by running a fixed effects regression to attribute part of the difference between the observed prices and the computed theoretical ones to the disaster wedge. Finally, based on a specific disaster type, I estimate the probability of the disaster for each country and day.

3.1 Data

I use yield curve and credit ratings data from Datastream, macroeconomic data from the International Monetary Fund's International Financial Statistics (IMF/IFS) and World Bank's World Development Indicators (WB/WDI), and conflict data from the Uppsala Conflict Data Program's Georeferenced Event Dataset (UCDP/GED).

3.1.1 Yield curve data

Refinitiv's Datastream provides daily government bond yields for a wide range of countries, including both developed and developing economies. The availability of bond data varies by country; more developed countries typically offer a greater variety of bonds and longer maturity horizons. The analysis includes 64 countries over various time horizons.¹⁴

I retrieved the daily "benchmark" yield curve, which is based on "benchmark" bonds.¹⁵ These are the most liquid government bonds, which are particularly relevant for analyzing investor expectations,

14. For a detailed list of all countries, including their respective time spans and maturity coverage, see Table C1 in the appendix.

15. These are based on Refinitiv Government Bond Indices, which are calculated using methodologies recommended by the European Federation of Financial Analysts Societies (EFFAS).

as they capture actively traded securities that swiftly respond to market developments.¹⁶ These cover standard government bonds with fixed rates and fixed maturity dates while excluding bonds with variable rates and other features that distort predictability.¹⁷ All the bonds are denominated in the local currency of the issuing country. I use the yield curve data provided directly by Refinitiv without any time lags.¹⁸

Finally, I restrict the sample to bonds with maturities between 1 and 10 years for two main reasons. First, this range aligns with the year-over-year growth rates of the macroeconomic variables. Second, these maturities are more frequently available in the dataset, ensuring adequate data coverage and consistency in the analysis.

3.1.2 Credit ratings data

Refinitiv's Datastream includes ratings from multiple credit rating agencies, such as Moody's, Fitch, Dominion Bond Rating Service (DBRS), and Rating & Investment (R&I). Additionally, it provides an equivalence mapping to the Standard & Poor's (S&P) rating scale, which consists of over 20 categories (e.g., AAA, AA+, AA, AA-, etc.).

To ensure consistency and comparability, I standardize all relevant ratings to their equivalent S&P categories. This transformation creates a unified scale for evaluating and aggregating ratings from different agencies. For each country and time period, the average rating is calculated as the mean of the S&P-equivalent ratings across all agencies.

3.1.3 Economic and conflict data

The economic variables of interest are consumption growth and inflation, which were obtained at a quarterly frequency from the IMF/IFS and an annual frequency from the WB/WDI. In both datasets, consumption growth is proxied by GDP growth in constant local currency units. Inflation is measured using the Consumer Price Index (CPI).

The IMF data, which provides quarterly updates, allows me to run the model at a quarterly frequency by inputting per-period consumption growth (G_t) and inflation (Π_t). I retrieve data for the 64 countries matching the financial data. In contrast, the annual World Bank data offers more comprehensive coverage over a longer time span, which is especially useful for estimating the parameters of the laws of motion for consumption growth and inflation, as well as the disaster parameters. This dataset includes 189 countries from 1989 to 2023.

Finally, to link economic effects to interstate wars, I utilize battle-related fatality data from the UCDP/GED. I aggregate this data to the country-year level. This dataset is essential for calibrating the

16. The Refinitiv Government Bond Indices include three main types: All Traded Index, which includes all eligible bonds, providing comprehensive market coverage; Tracker Index, a sample of bonds that closely tracks overall market performance; and Benchmark Index, focusing on the most liquid bonds.

17. Excluded bonds include those with inflation-linked, floating rate, convertible, and bonds with embedded options or warrants.

18. Refinitiv also offers computed yield curves for third parties, which may have pricing lags.

“jumps” associated with wars in the model’s parameters. This includes 180 countries from 1989 to 2023.

3.2 Calibration

Calibrating the model for all countries requires setting parameters for the utility function, the laws of motion for consumption growth and inflation, and disaster-related parameters. See Table 1 and Table 2 for a summary of the calibration.

3.2.1 Utility function and laws of motion

I derive the utility function parameters from established literature. Following the methodology posited by Barro (2006), I set the discount factor, β , to 0.97 per year, and the coefficient of relative risk aversion, θ , to 4, which are common to all the countries.

Table 1: Summary of calibration: utility function and laws of motion

Variable	Value	Source
Time preference (β)	0.97	Barro (2006)
Risk aversion (θ)	4	Barro (2006)
Consumption growth (G_{ct})	Country-specific	IMF/IFS
Inflation (Π_{ct})	Country-specific	IMF/IFS
Constant of consumption growth ($\alpha_{G,c}$)	Country-specific	Estimated from WB/WDI
Constant of inflation ($\alpha_{\Pi,c}$)	Country-specific	Estimated from WB/WDI
Persistence of consumption growth ($\phi_{G,c}$)	Country-specific	Estimated from WB/WDI
Persistence of inflation ($\phi_{\Pi,c}$)	Country-specific	Estimated from WB/WDI
S.d. of consumption growth ($\sigma_{\varepsilon,c}$)	Country-specific	Estimated from WB/WDI
S.d. of inflation ($\sigma_{\eta,c}$)	Country-specific	Estimated from WB/WDI

Notes: This table presents the calibration of the utility function and laws of motion. The laws of motion for consumption growth and inflation are estimated using OLS on country-specific time series data from WB/WDI.

Sources: Barro (2006), IMF/IFS, WB/WDI, and author’s calculations.

The laws of motion for consumption growth and inflation are represented by Equation 8 and 10. Taking logs transforms the laws of motion into a linear form, which, in the absence of disaster shocks, follows an AR(1) process. For each country c , I estimate the constant parameters ($\alpha_{G,c}$ and $\alpha_{\Pi,c}$), the persistence parameters ($\phi_{G,c}$ and $\phi_{\Pi,c}$), and the standard deviations ($\sigma_{\varepsilon,c}$ and $\sigma_{\eta,c}$) using OLS on WB/WDI time series from 1989 to 2023. The distribution of the estimated parameters shows that the constant parameters are around 1.02 for both variables. Both log consumption growth and log inflation exhibit mean reversion. The inflationary process is more persistent, with an average persistence of 0.5, compared to 0.2 for consumption growth. See Figure B1 in the appendix for kernel density plots of

these estimates. For the period-specific consumption growth and inflation, G_{ct} and Π_{ct} , I use quarterly year-over-year data from IMF/IFS.

With all these parameters, I can compute the theoretical non-disaster prices, \hat{Q}_{Nct}^{ND} , for each maturity N , country c , and period t . As only G_{ct} and Π_{ct} vary over time, the non-disaster price is updated quarterly. See Table 1 for a summary of the calibration of the utility function and the laws of motion.

3.2.2 Disaster parameters

The disaster parameters to be calibrated include the jumps in consumption growth (J_G) and inflation (J_Π), the probability of default during a disaster (γ), and the haircut size (J_F). These parameters are calibrated specifically for each type of disaster and are the same for all countries. I define two types of disasters: interstate war and sovereign default.

For interstate war, I conducted a two-way fixed effects analysis using WDI/WB data.¹⁹ The results show that a year in war reduces consumption growth by 2% and increases inflation by 2%. Therefore, I set $J_G = 0.98$ and $J_\Pi = 1.02$. The regression results are presented in Table C2 in the appendix. I set J_F , to 0.56, based on the haircut analysis from Luckner et al. (2023), which uses historical data on sovereign defaults triggered by geopolitical disasters. Given that they recorded 45 defaults resulting from 95 interstate wars, I set the probability of default γ to 0.5.

For sovereign default, the objective is to capture the probability of default using $\delta_{1,t}$. Thus, the conditional probability of default given a disaster, γ , becomes redundant, so I set it to 1. The parameter J_F is set to 0.44, as the average haircut for sovereign defaults is 44% (Meyer, Reinhart, and Trebesch 2022). The jumps in consumption growth and inflation are set to 1.

Table 2: Summary of calibration: disaster parameters by disaster type

Disaster type	J_G	J_Π	γ	J_F	Source
Interstate war	0.98	1.02	0.5	0.56	Von Laer & Bartels (2023), author's calculations
Sovereign default	1	1	1	0.44	Meyer et al. (2022)

Notes: This table presents the calibration of disaster parameters by disaster type. J_G and J_Π are the jumps in consumption growth and inflation, respectively. γ is the probability of default when a disaster occurs, and J_F is the haircut size. $\phi_\delta = 0.5$ for all disaster types.

Source: Barro (2006), Luckner et al. (2023), and Meyer, Reinhart, and Trebesch (2022) and author's calculations on WB/WDI and UCDP/GED data.

Based on the calibrated disaster parameters and laws of motion, I can compute the overall jump, $\hat{J}_{\tau,cN}$, using Equation 16. The persistence parameter of the disaster probability, ϕ_δ , is set to 0.5 for all disaster types. Table 2 summarizes the calibration for each disaster.

19. To match the conflict size with Luckner et al. (2023), I define war as having more than 1,000 deaths per year using UCDP data.

Figure 1 shows the simulated impact of varying $\delta_{1,ct}$ values for each disaster type on the price curve, based on the U.S. calibration. The likelihood of either interstate war or default leads to a price drop across all maturities. For interstate war, the inflationary and default risks outweigh the recessionary effects, causing the decline in prices. Default has a stronger negative impact.

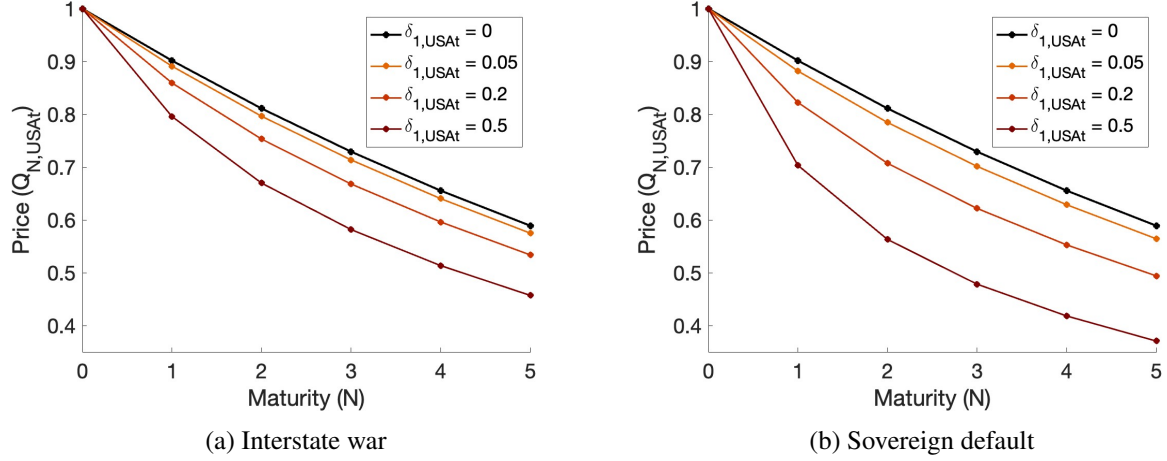


Figure 1: Comparative Statics of Disaster Probabilities

Notes: The figure presents simulated price curves for each disaster type, calibrated for the US with varying disaster probabilities, $\delta_{1,ct}$. The persistence parameter is set to $\phi_\delta = 0.5$, and other disaster parameters are from Table 2. I set $G_t = \Pi_t = 1.02$.
Source: Author's calculations.

3.3 Bringing the model to the data

Building on the calibration, I bring the theoretical model to the data to estimate investors' perceived probability of disaster. Incorporating the panel structure using the country index c and taking logs, Equation 14 transforms into

$$q_{Nct} = q_{Nct}^{ND} + \sum_{\tau=1}^N \log (1 + \phi_\delta^{\tau-1} \delta_{1,ct} (J_{\tau,cN} - 1)) \quad (18)$$

with $q_{Nct} = \log(Q_{Nct})$ and $q_{Nct}^{ND} = \log(Q_{Nct}^{ND})$. The difference between the observed log price and the theoretical log price captures the disaster wedge. I bring this equation to the data by employing a fixed effects regression specified as:

$$q_{Nct} = \beta \hat{q}_{Nct}^{ND} + \kappa_{Nc} + \kappa_{Nt} + \kappa_{ct} + u_{Nct} \quad (19)$$

where κ_{Nc} , κ_{Nt} and κ_{ct} represent fixed effects for country-maturity, maturity-time, and country-time interactions, respectively, and u_{Nct} is the error term. q_{Nct} is the observed log price of a bond sourced from Datastream. \hat{q}_{Nct}^{ND} is the computed non-disaster theoretical log price derived from the model's calibration. While observed bond prices are available daily, the computed theoretical prices are updated

quarterly based on economic data. To align frequencies, I interpolate the quarterly theoretical prices to a daily level. The results are robust when using the quarterly model, which uses quarterly averages of observed prices.

This equation suggests that observed bond prices can be explained by the non-disaster theoretical price, which reflects expectations based on the current business cycle, plus a set of unobserved factors varying at different levels. Fixed effects regression offers several advantages. First, it corrects for potential model misspecifications. Comparing Equation 18 with the regression equation, if the model perfectly captures the bond price data-generating process, $\hat{\beta}$ would approximate 1. However, allowing it to deviate provides a more accurate reflection of the relationship and serves as a measure of model fit. Second, because $\delta_{1,ct}$ varies at the ct level, the model's country-time interaction term, κ_{ct} , isolates variations in country-specific factors over time, which is essential for estimating disaster probabilities. Finally, the additional fixed effects address structural and temporal influences, which enhance identification. The country-maturity interaction term, κ_{Nc} , captures structural yield curve differences across countries, reflecting time-stable variations potentially due to regulatory or market-specific conditions. The maturity-time interaction term, κ_{Nt} , controls for maturity-specific factors impacting all countries in a given period, such as global shifts in demand for certain maturities or adjustments in term premiums.

Table 3: Fixed effect regression

	Observed price (q_{Nct})				
	(1)	(2)	(3)	(4)	(5)
Non-disaster price (\hat{q}_{Nct}^{ND})	0.109*** (0.001)	0.206*** (0.001)	0.218*** (0.0004)	0.312*** (0.0002)	0.292*** (0.0002)
Country-time FE	✓	✓	✓	✓	✓
Maturity-country FE	✓	✓			
Maturity-time FE	✓		✓		
Observations	1,765,539	1,765,539	1,765,539	1,765,539	1,766,001
Adjusted R ²	0.973	0.946	0.850	0.831	0.350

Note: This table presents a fixed effects regression of the observed log bond price ($q_{Nct} = \log(Q_{Nct})$) on the log of the theoretical non-disaster price ($q_{Nct}^{ND} = \log(Q_{Nct}^{ND})$). Fixed effects are κ_{Nc} (Maturity-country), κ_{Nt} (Maturity-time), and κ_{ct} (Country-time). Models differ by their inclusion of these fixed effects. Robust standard errors are reported in parentheses, with * $p < 0.1$, ** $p < 0.05$, and *** $p < 0.01$ indicating significance levels.

Source: Datastream data for observed prices, and theoretical prices are calculated based on WB/WDI and IMF/IFS data.

Table 3 presents the regression results from different specifications, which vary in the fixed effects included. The favorite specification, from which I estimate the disaster probabilities, includes all fixed effects. Across all specifications, $\hat{\beta}$ is positive and significant, showing that the theoretical price moves in the same direction as observed prices. However, the values are below 1 in all specifications and generally decrease as more fixed effects are added—from 0.316 (only κ_{ct}) to 0.108 (with all fixed effects).²⁰ This pattern supports including additional fixed effects to capture unobserved factors beyond the the-

20. Given that bond prices are close to 1, a $\hat{\beta}$ on log prices of 0.1 does not indicate major deviations.

oretical model, enhancing model fit as indicated by the significant increases in the adjusted R^2 with each additional fixed effects interaction. Almost identical results are found when using the quarterly frequency model, see Table C3 in the appendix.

Given that $\delta_{1,ct}$ varies at the country-time level, it is captured in $\hat{\kappa}_{ct}$ as the common unobserved factor at the ct level. Its interpretation is as follows: if $\hat{\kappa}_{ct}$ is significantly positive, it indicates that there is an unobserved factor at the country-time level causing bond prices to be higher than what the current business cycle, and the other factors controlled by the other fixed effects, would suggest. Conversely, a significantly negative $\hat{\kappa}_{ct}$ implies that this unobserved factor is reducing bond prices. Since disaster risk reduces bond prices across maturities, as shown in Figure 1, a negative $\hat{\kappa}_{ct}$ may indicate that the unobserved factor is disaster risk.

Figure 2 illustrates the evolution of $\hat{\kappa}_{ct}$ for six representative countries selected for their distinct levels of disaster risk. Germany and the United States represent stable countries with no significant disaster risk. Ireland and Spain exemplify relatively stable countries that experienced periods of disaster risk (default risk during the European debt crisis) that ultimately did not materialize. In contrast, Greece and Ukraine represent countries where disaster risk materialized, including Greece's default in 2012 and Ukraine's interstate conflict in 2023. The horizontal lines at 0 and -0.5 serve as reference thresholds to facilitate comparison of $\hat{\kappa}_{ct}$ values across countries.

Stable countries with no significant disaster risk, such as Germany and the USA, generally exhibit $\hat{\kappa}_{ct}$ values that remain positive or only briefly touch the zero baseline. This pattern extends to other economically robust regions, including Australia, the United Kingdom, Scandinavian countries (e.g., Sweden, Norway, Denmark), and stable European economies like Austria, the Netherlands, and Switzerland. Likewise, leading Asian economies such as Japan, South Korea, and Singapore also display this pattern.

Relatively stable countries that experienced periods of known disaster risk, such as Ireland and Spain, typically display positive $\hat{\kappa}_{ct}$ values with only shallow dips into negative territory during times of financial instability. Ireland's lowest $\hat{\kappa}_{ct}$ point occurs in mid-2011, aligning with austerity measures and bailout negotiations during the peak of the European debt crisis. Spain similarly reaches a minimum in mid-2012, reflecting peak financial strain in this period. Comparable patterns are seen in other southern European countries, including Portugal, Italy, and Cyprus. Other notable examples of brief negative dips without crossing the -0.5 threshold include Israel during the Second Intifada, amid severe conflict and economic disruption, and Poland in 2002, during economic adjustments following rapid liberalization and structural reforms, which led to rising unemployment, social discontent, and fiscal strain. Additionally, countries like Mexico and India experienced multiple brief dips into negative territory, indicating episodic financial pressures without prolonged instability.

In contrast, Greece and Ukraine exhibit severe declines in $\hat{\kappa}_{ct}$ leading up to their respective disasters, with values reaching their lowest points and crossing well below the -0.5 threshold as the disasters unfolded. Greece's significant drop aligns with its 2012 default during the European debt crisis, while Ukraine's plunge reflects the escalation of interstate conflict in 2023. Other severe declines are observed

in Sri Lanka and Ghana in 2022, coinciding with their defaults during severe economic and political instability.

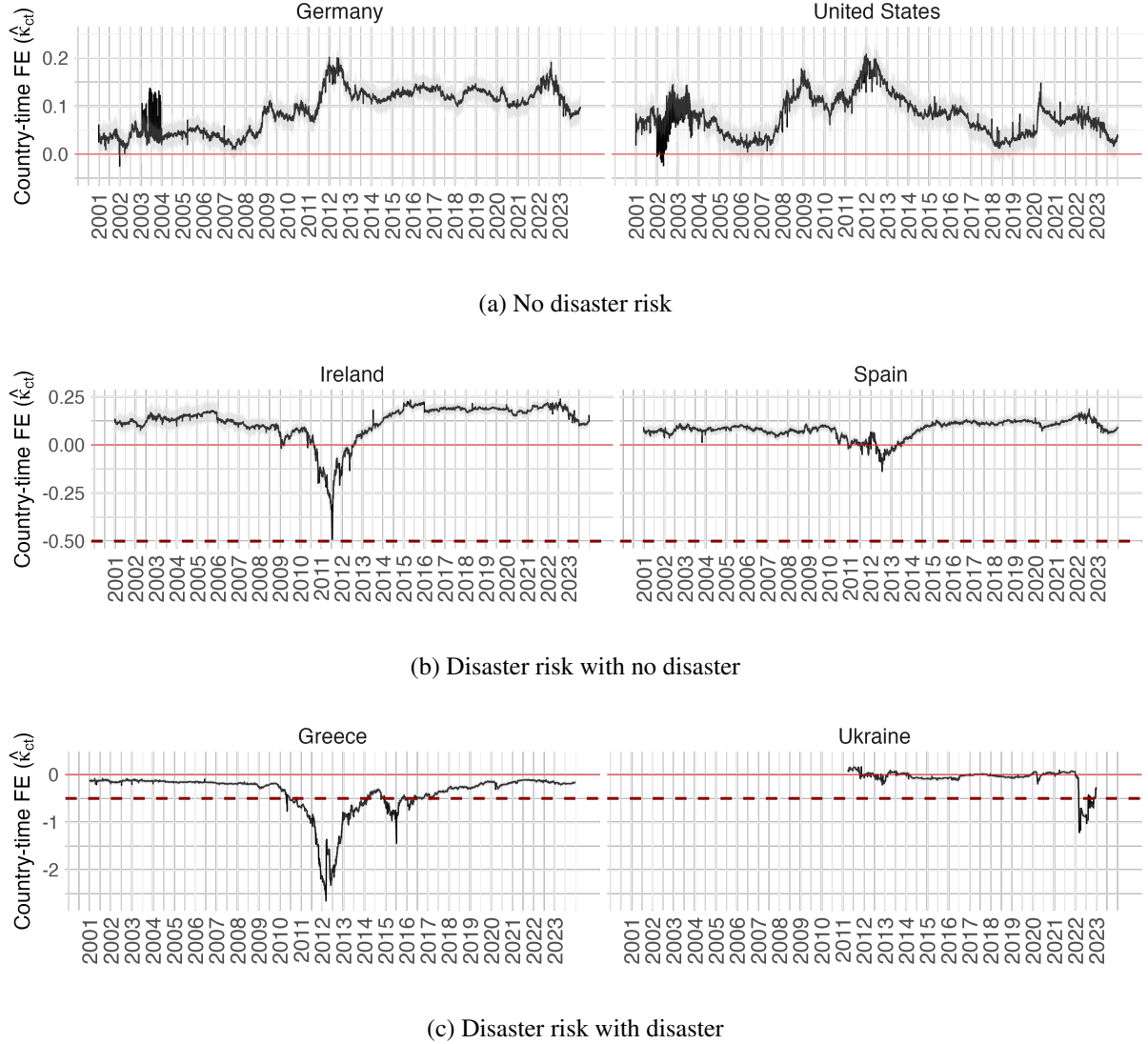


Figure 2: Evolution of $\hat{\kappa}_{ct}$ for selected countries

Notes: The figure shows the evolution of $\hat{\kappa}_{ct}$ with 95% confidence intervals for selected countries: Germany, the United States, Ireland, Spain, Greece, and Ukraine. The red lines at 0 and -0.5 represent reference thresholds.

Source: Author's calculations.

These patterns suggest that when $\hat{\kappa}_{ct}$ values dip into the negative range, investors may be factoring in disaster risk. Figure B2 in the appendix compares the daily and quarterly models for estimating $\hat{\kappa}_{ct}$. The daily model captures more detailed variation along the same overall trend as the quarterly model. For the evolution of $\hat{\kappa}_{ct}$ across the full set of countries, see Figures B3, B4, B5, and B6 in the appendix.

To derive disaster probabilities, I assume $\hat{\kappa}_{ct}$ corresponds to the disaster wedge. Specifically, $\hat{\kappa}_{ct}$

represents the average effect of disaster wedges across all maturities, i.e.,

$$\hat{\kappa}_{ct} = \frac{\sum_{N \in \mathcal{N}(c,t)} q_{Nct} - \hat{\beta} \hat{q}_{Nct}^{ND} - \hat{\chi}_N - \hat{\kappa}_{Nc} - \hat{\kappa}_{Nt}}{|\mathcal{N}(c,t)|} \quad (20)$$

where $\mathcal{N}(c,t)$ is the set of maturities available for country c at time t , and $|\mathcal{N}(c,t)|$ is the number of them. The theoretical model then implies

$$\hat{\kappa}_{ct} = \frac{\sum_{N \in \mathcal{N}(c,t)} \sum_{\tau=1}^N \log(1 + \phi_{\delta}^{\tau-1} \delta_{1,ct} (J_{\tau,cN} - 1))}{|\mathcal{N}(c,t)|}$$

Finally, I specify the type of disaster by inputting the estimated persistence parameter ($\hat{\phi}_{\delta}$) and the overall jump effect of the disaster ($\hat{J}_{\tau,cN}$) into the previous equation, leaving $\delta_{1,ct}$ as the only variable to be determined. The type of disaster is tailored to each country's context; for example, an interstate war is specified for Ukraine, while a sovereign default is specified for Greece. Given that the shortest maturity bond available is a one-year bond, $\delta_{1,ct}$ corresponds to the probability of a disaster occurring within one year.

I estimate $\delta_{1,ct}$ by minimizing the squared difference between $\hat{\kappa}_{ct}$ and the theoretical form of the disaster wedge:

$$\hat{\delta}_{1,ct} = \underset{\delta_{1,ct}}{\operatorname{argmin}} \left(\hat{\kappa}_{ct} - \frac{\sum_{N \in \mathcal{N}(c,t)} \sum_{\tau=1}^N \log(1 + \hat{\phi}_{\delta}^{\tau-1} \delta_{1,ct} (\hat{J}_{\tau,cN} - 1))}{|\mathcal{N}(c,t)|} \right)^2$$

4 Results

Using the process explained in the previous section, I estimate investors' perceived probability of disaster for each country and day. To assess their predictive value, I first analyze how these probabilities evolve leading up to the disaster events. Second, I explore their relationship with credit ratings. Finally, I conduct a series of forecasting exercises using machine learning techniques to evaluate the added value of the estimated disaster probabilities. I assess whether these probabilities enhance the prediction of downgrades, upgrades, and disaster events relative to a model that uses only credit ratings data.

4.1 Disaster probabilities before disasters

4.1.1 Sovereign defaults: Greece, Ghana, and Sri Lanka

Figure 3 shows the evolution of Greece's sovereign default probability during the European debt crisis, spanning from the deficit revelation in late 2009 to the execution of the Private Sector Involvement (PSI) agreement in March 2012. Key events are marked by dashed vertical lines. The probability rose sharply from 25% after late 2009 when the Greek government admitted its budget deficit was far higher than previously reported. Austerity measures were implemented, but at least an immediate impact is not

observed. In April 2010, the default probability spiked dramatically from 40% to 60%. It then declined to 50% in May 2010, coinciding with the announcement of a €110 billion EU-IMF bailout package. However, this relief was short-lived, as the probability rose again above 70%, before falling back to 50%, aligning with the establishment of the European Financial Stability Facility (EFSF). The EFSF, a temporary crisis resolution mechanism, aimed to support Eurozone countries in distress by issuing bonds backed by guarantees from member states. Protests against austerity measures in May 2010 marked the beginning of a new, slow but steady increase in default probability, rising from 50% to 100% by June 2011. In July 2011, the EU announced a second bailout package that included a plan for voluntary debt restructuring. On the day of the announcement, the probability dropped by 20%. However, it quickly returned to 100% and remained elevated until the PSI agreement was finalized. The PSI included a 50% haircut for private bondholders, but it was not until March 2012 that it was fully executed.

This case highlights the accuracy of financial markets in predicting sovereign default and their rapid reaction to new information and policy measures. The figure suggests that bailouts and international mechanisms have an immediate impact on default probabilities, while austerity measures alone do not.

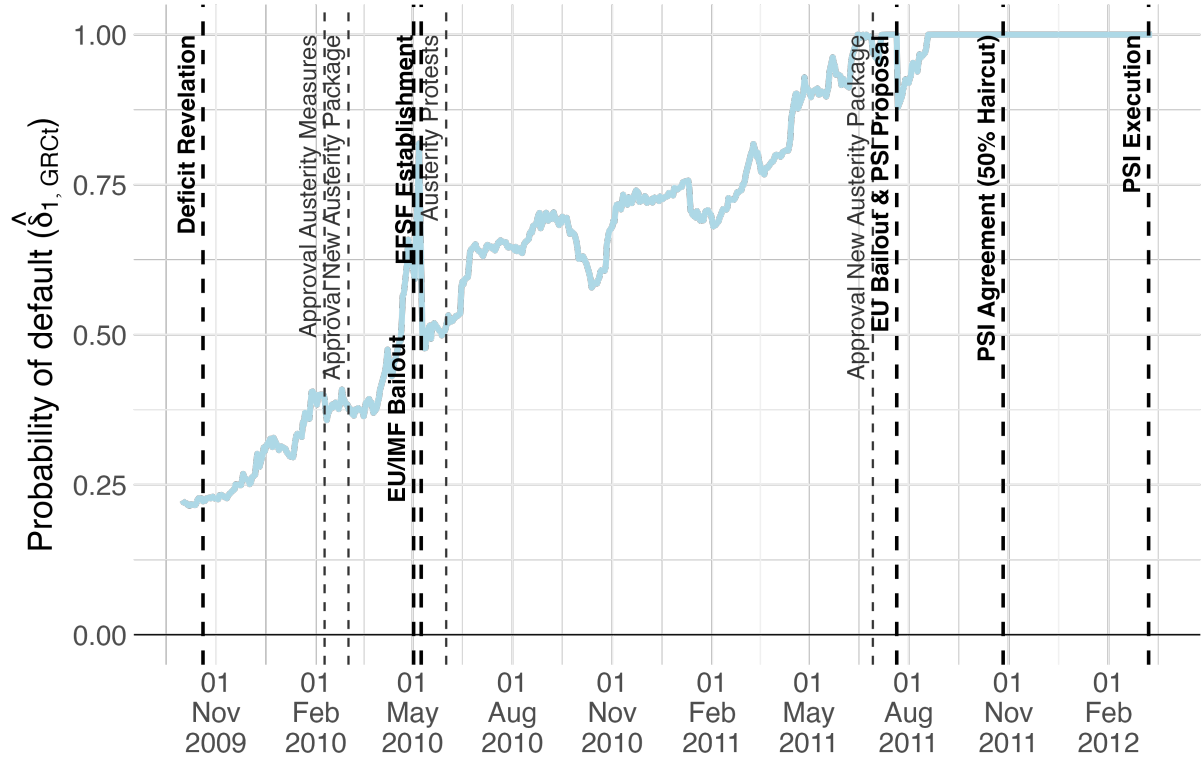


Figure 3: Evolution of probability of default for Greece

Notes: The figure shows the evolution of the probability of a sovereign default for Greece. Vertical lines represent relevant events.

Source: Author's calculations.

Figure 4 tracks Ghana's rising default probability from May 2018 to its official default in December 2022. The trajectory resembles Greece's case, as the probability of default steadily rises from 30%

to 100% over several years. However, Ghana's experience includes fewer notable interventions. In May 2018, the probability of default stood at 30% and increased steadily to around 60% by the end of 2020. The COVID-19 lockdown caused a temporary spike in default probability, but it stabilized at approximately 60% thereafter. It was not until May 2022, when the Ghanaian government dismissed the possibility of seeking assistance from the IMF, that the probability sharply increased, eventually reaching 100%. Once the probability peaked at 100%, the government reversed its stance and began discussions with the IMF. Despite this shift, no immediate agreement was reached, and the probability remained at the 100% level. Toward the end of 2022, the government announced plans for a local debt restructuring, followed shortly by a declaration of default on foreign debt.

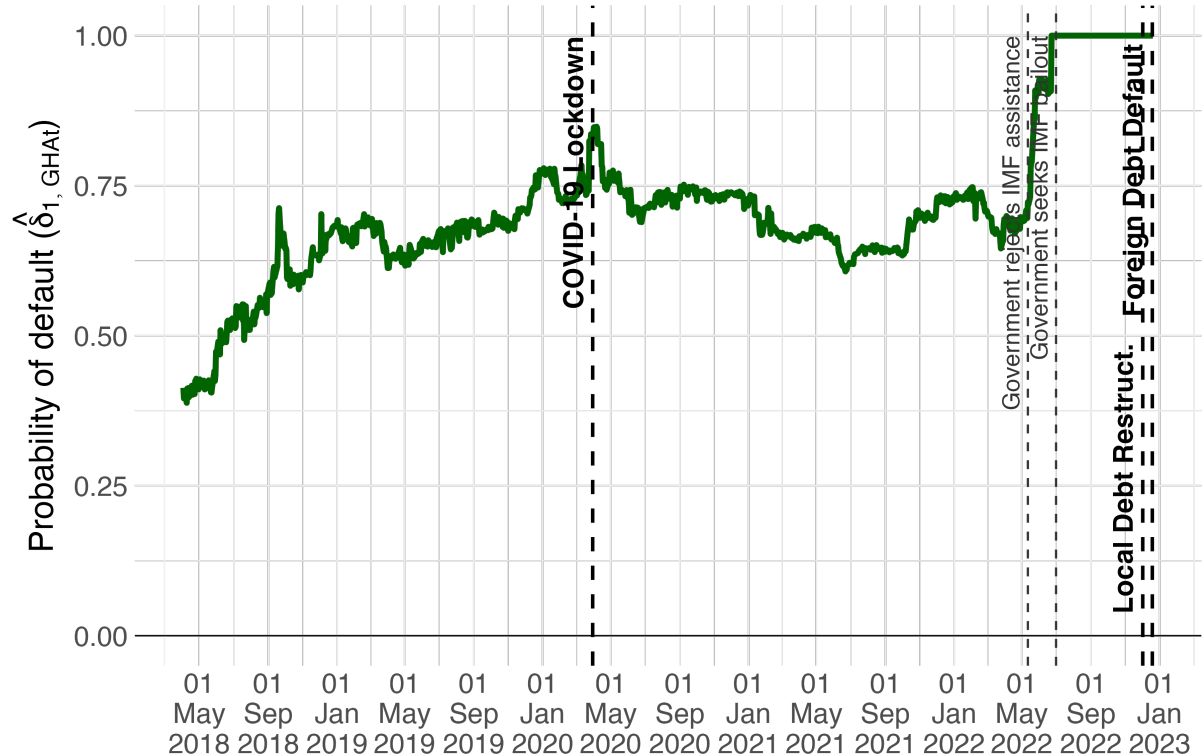


Figure 4: Evolution of probability of default for Ghana

Notes: The figure shows the evolution of the probability of a sovereign default for Ghana. Vertical lines represent relevant events.

Source: Author's calculations.

Figure 5 depicts the probability of default for Sri Lanka from January 2022 to the declaration of default on foreign debt in April 2022. In February 2022, investors assigned a near-zero probability of default to Sri Lanka. This began to change in March, following a public statement by the IMF declaring Sri Lanka's debt unsustainable. Probability rose to 20% thereafter. Mass protests erupted, and a state of emergency was declared, keeping the probability stable around 20%. In the days leading up to the default, the probability surged to approximately 40%, and on the day of the default, it spiked further to 60%.

Although the probability did not reach 100%, the rapid increases leading up to the default provide clear evidence of investors' short-term anticipation of the crisis. This underscores the responsiveness of financial markets to developments even in short time frames.

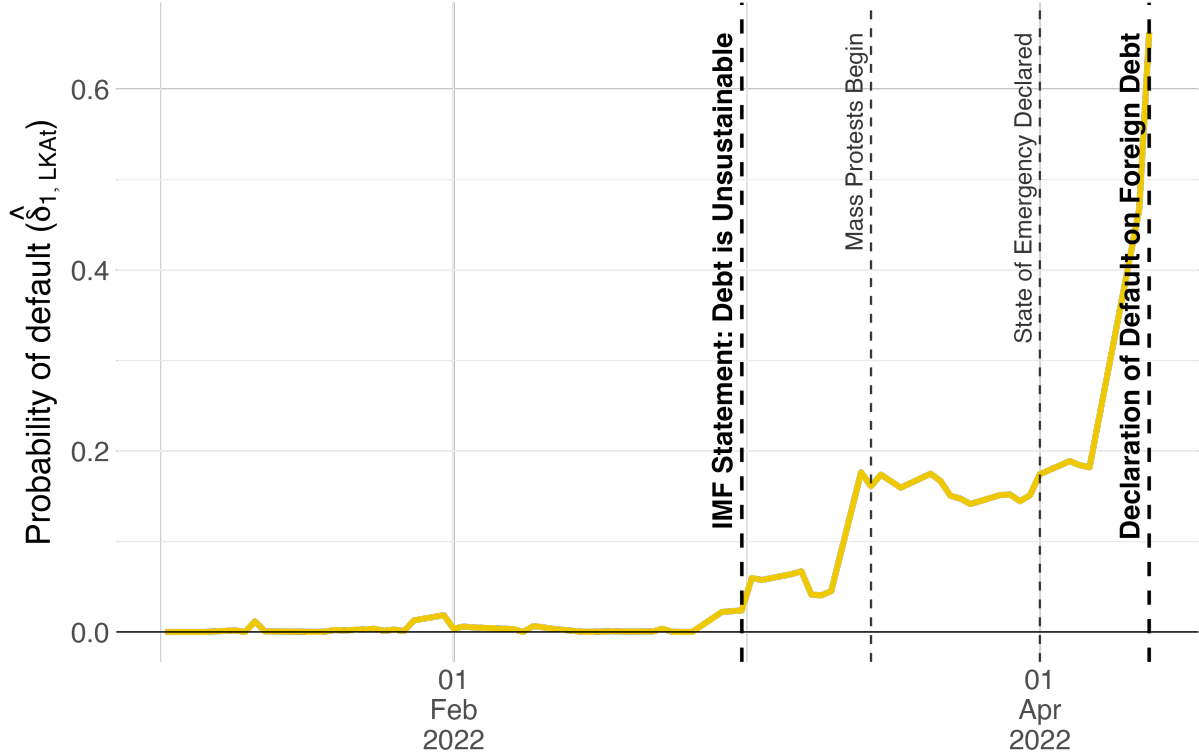


Figure 5: Evolution of probability of default for Sri Lanka

Notes: The figure shows the evolution of the probability of a sovereign default for Sri Lanka. Vertical lines represent relevant events.

Source: Author's calculations.

4.1.2 Interstate war: Ukraine and Russia

Figure 6 illustrates the evolution of the estimated probability of an interstate war in Ukraine and Russia, from December 2021 to March 2022. Investors assigned virtually no probability to an interstate war until approximately two months before the conflict. Starting in January, their perception of war risk began to shift, with the probability of conflict in the two countries rising gradually to around 20%. Notably, even after Belarus's military drills on February 10 and Russia's recognition of the independence of Donetsk and Luhansk on February 21, investors' probability of a conflict remained relatively steady. It was only after the invasion commenced on February 24 that the estimated probability of interstate jump to over 90%. This finding suggests that the market was indeed anticipating for the risk of conflict prior to its onset.

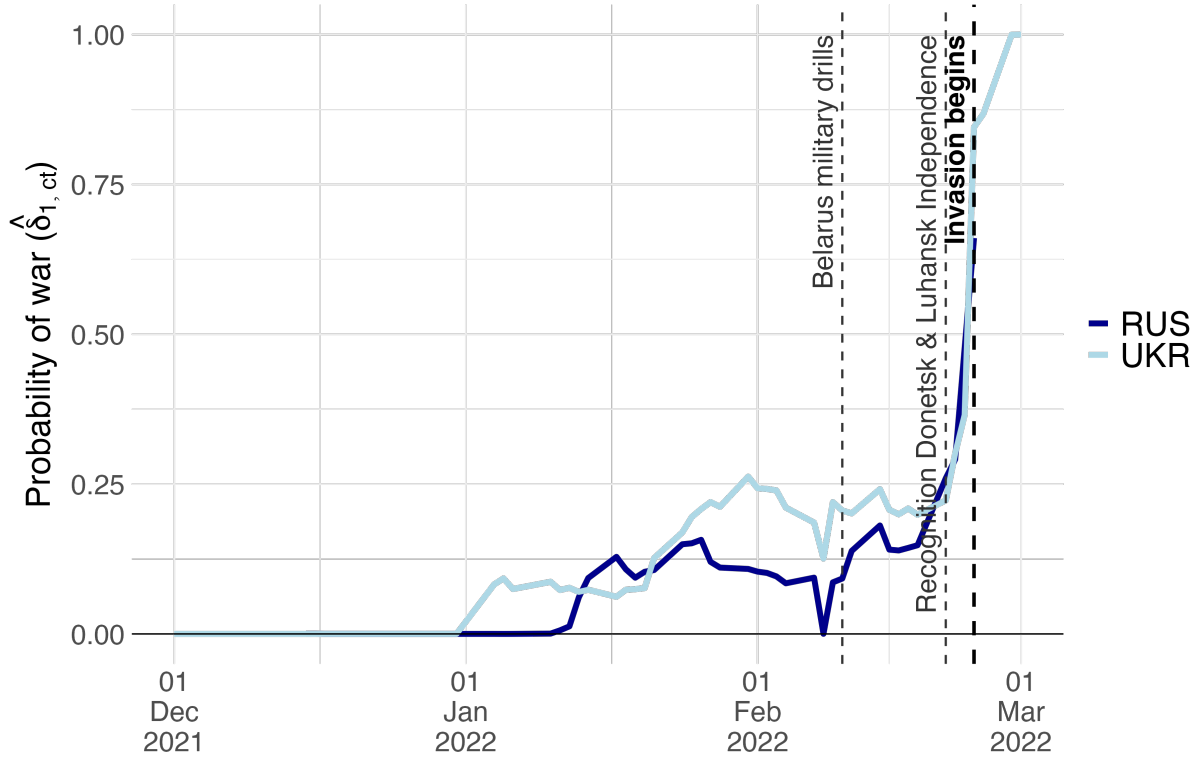


Figure 6: Evolution of probability of interstate war for Russia and Ukraine

Notes: The figure shows the evolution of the probability of an interstate war for Russia and Ukraine. Vertical lines represent relevant events.

Source: Author's calculations.

4.2 Disaster probabilities and credit ratings

I analyze their relationship with an established measure of default risk, such as credit ratings. Credit ratings are qualitative measures of a borrower's creditworthiness, reflecting the likelihood of default. Ratings incorporate a broad range of factors, including public debt levels, fiscal deficits, economic growth, political stability, and governance quality. Given that the disasters analyzed involve sovereign defaults and interstate wars—where default risk is the dominant factor—this comparison is appropriate. For this exercise, I use monthly averages of the estimated probabilities.

Figure 7 presents a boxplot of the estimated disaster probabilities across credit rating categories, each representing a subset of rating values. The boxplot illustrates the distribution of the probabilities, with the black line representing the median, the blue box indicating the interquartile range (25th to 75th percentiles), and the bars extending to the 10th and 90th percentiles. For ratings from AAA to B, the median of the default probabilities remains at 0%, with a compressed distribution reflecting the concentration of developed countries with minimal default risk. In contrast, the median of the probabilities rises to 30% for CCC+ to CC- ratings, showing significant variation in the distribution, and exceeds 90% for ratings from C+ to RD, where the distribution is concentrated at the upper end. The relationship between

ratings and default probabilities is positive and notably non-linear. The AAA to B category encompasses the majority of rating values—approximately 80%—indicating a disproportionate concentration of low-risk ratings. The grouping of ratings into these categories is based on the S&P study (Rossi, Kraemer, and Singh 2023), which calculates sovereign default probabilities for each group based on observed transition frequencies. For ratings ranging from AAA to BB, the one-year default probabilities are near zero, with AAA at 0% and B at 4%. A sharp increase to 50% is observed when ratings fall within the CCC to CC category, while no data is reported for the C category. The figure demonstrates that the model’s estimated probabilities align closely with the S&P findings.

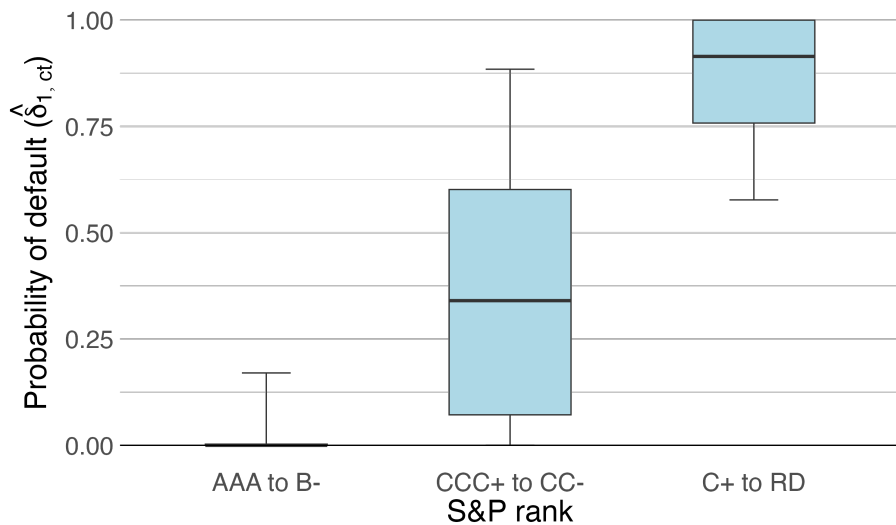


Figure 7

Notes: The figure shows a boxplot of the estimated disaster probabilities by credit rating category. The boxplot illustrates the distribution of the probabilities, with the black line representing the median, the blue box indicating the interquartile range (25th to 75th percentiles), and the bars extending to the 10th and 90th percentiles.

Source: Author’s calculations.

4.3 Predictive value of the estimated disaster probabilities

I assess whether they enhance the prediction of downgrades, upgrades, and disaster events relative to a model that uses only credit ratings data. To do this, I forecast future downgrades, upgrades, and disasters using three models: one using only disaster probabilities, another using only credit rating variables, and a third combining both sources. Credit rating variables include the current rating, the magnitude of last downgrade and upgrade, and the time since the last downgrade and upgrade.

For all exercises, I use an expanding window forecasting method with a monthly frequency. This approach starts with an initial dataset to estimate the model and predict out-of-sample values. Over time, more data is added incrementally, the model is re-estimated, and predictions are made for the next period. This simulates a real-time forecasting scenario, where predictions are based on all available data up to the present, and as time progresses, newly available data is incorporated into the model.

To evaluate the predictive performance of the models, I use two standard metrics: the ROC curve and the PR curve. The ROC curve plots the true positive rate (TPR) against the false positive rate (FPR) across different classification thresholds.²¹ The TPR represents the proportion of actual positive events correctly identified relative to the total number of actual positive events, while the FPR indicates the proportion of negative events incorrectly classified as positive relative to the total number of actual negative events. The ROC-AUC summarizes this curve into a single value, where 1.0 represents perfect discrimination and 0.5 indicates performance equivalent to random guessing. A higher ROC-AUC reflects the model's ability to effectively distinguish between positive and negative outcomes across all thresholds. In contrast, the PR curve evaluates the balance between precision (the proportion of correctly predicted positive events out of all predicted positives) and recall (the proportion of actual positive events correctly identified).²² The ROC curve evaluates performance across all thresholds and is generally preferred for assessing overall discrimination. The PR curve focuses on the positive class, making it valuable when the focus is on positives and class imbalance is present.

4.3.1 Forecasting downgrades and upgrades

The objective is to forecast downgrades and upgrades in the next month. All models use a Random Forest, a technique that builds multiple decision trees, aggregates their predictions, and effectively handles non-linear relationships and complex interactions.²³

Figure 8 illustrates the predictive performance of the three models for forecasting downgrades: using only disaster probabilities, using only credit rating variables, and combining both sources. While the disaster probability model performs reasonably well, achieving ROC-AUC and PR-AUC scores of 0.74 and 0.05 respectively, the credit ratings model performs better, with scores of 0.84 and 0.14. The combined model significantly improves predictive performance, with a ROC-AUC of 0.88 and a PR-AUC of 0.26. The combination of disaster probabilities, which act as forward-looking indicators, and credit ratings, which encapsulate historical and structural information, creates a more comprehensive predictive framework. This improvement highlights the complementary nature of these data sources. The disparity between high ROC-AUC and low PR-AUC reflects the challenges posed by imbalanced datasets, where models struggle with precision and recall because events are rare.

Figure 9 illustrates the predictive performance of the three models for forecasting upgrades. Disaster probabilities and credit ratings perform worse than for downgrades, with ROC-AUCs of 0.6 and 0.7, respectively. Again, the model using credit ratings performs better, though the PR-AUC remains extremely low for both models. The combined model achieves the ROC-AUC of 0.66 and the PR-AUC

21. TPR, also known as sensitivity, is defined as $TPR = \frac{\text{True Positives}}{\text{True Positives} + \text{False Negatives}}$. FPR is defined as $FPR = \frac{\text{False Positives}}{\text{False Positives} + \text{True Negatives}} = 1 - \text{Specificity}$.

22. Precision is defined as $Precision = \frac{\text{True Positives}}{\text{True Positives} + \text{False Positives}}$. Recall is equivalent to TPR.

23. The Random Forest model is parameterized with 500 trees, 6 variables randomly selected at each split, and variable importance enabled. Trees are grown to their maximum depth, with a minimum of 1 observation per terminal node.

remains at 0.03. The combined model does not result in a significant improvement in this regard. The lower PR-AUC and the pronounced scaling of the ROC curve show that there are very few upgrades.

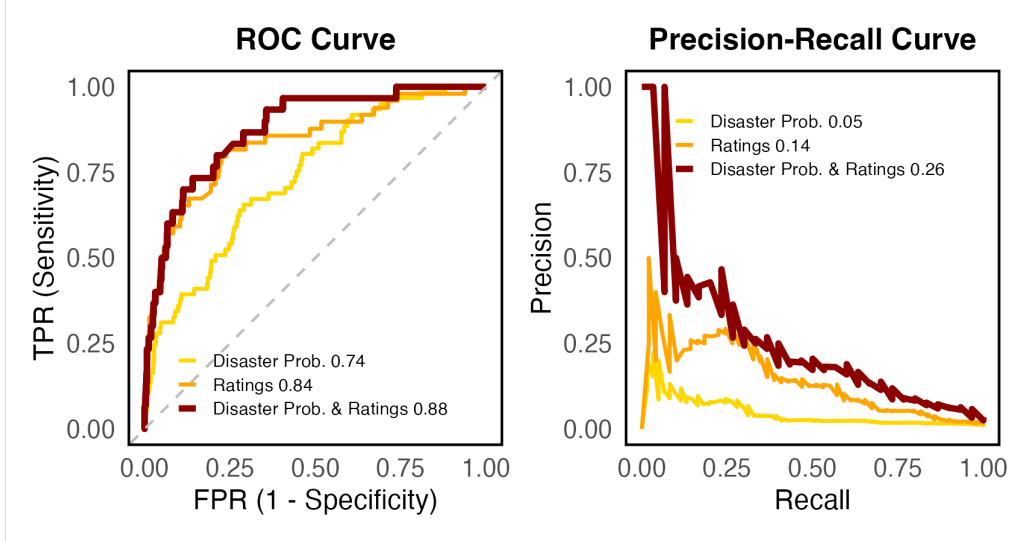


Figure 8: Predictive performance of disaster probabilities and credit ratings for downgrades

Notes: The figure shows the predictive performance of three different models for forecasting downgrades: using only disaster probabilities, using only credit rating variables (including the current rating, the magnitude of the last downgrade and upgrade, and the time since the last downgrade and upgrade), and using both sources. All models use a Random Forest with an expanding window forecasting method.

Source: Author's calculations.

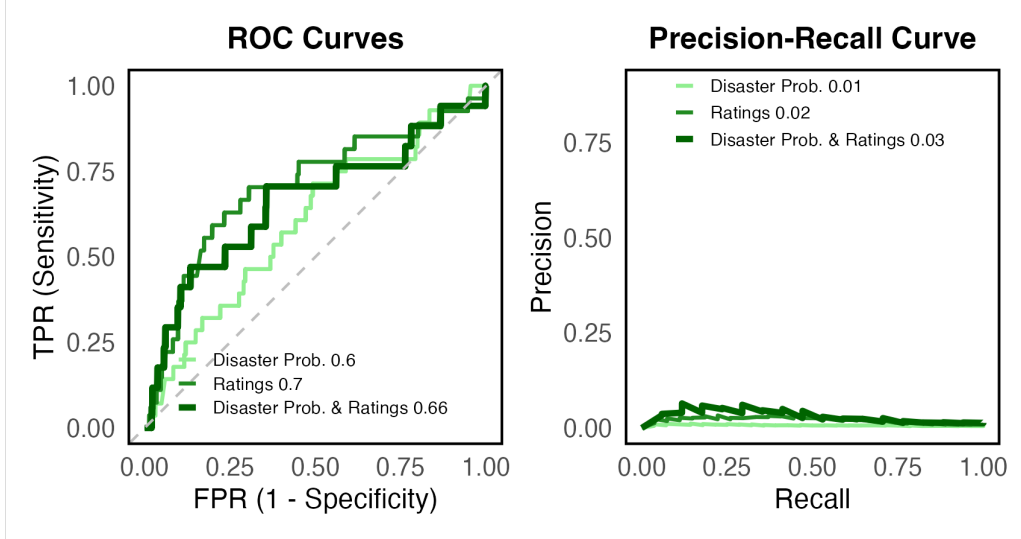


Figure 9: Predictive performance of disaster probabilities and credit ratings for upgrades

Notes: The figure shows the predictive performance of three different models for forecasting upgrades: using only disaster probabilities, using only credit rating variables (including the current rating, the magnitude of the last downgrade and upgrade, and the time since the last downgrade and upgrade), and using both sources. All models use a Random Forest with an expanding window forecasting method.

Source: Author's calculations.

4.3.2 Forecasting disaster events

The objective is to forecast disasters occurring within one year. The key difference here is that when using disaster probabilities alone, they are applied directly in the forecasting exercise without the Random Forest, as they inherently represent the probability of a disaster. When using only credit rating variables and the combined approach, I apply the same Random Forest model as in previous exercises.

Figure 10 shows the predictive performance of the three models for forecasting disasters. Disaster probabilities perform reasonably well, achieving an AUC of 0.79 for the ROC curve and 0.24 for the PR curve. The Random Forest model utilizing credit ratings performs significantly better, with a ROC-AUC of 0.94 and a PR-AUC of 0.76. Notably, integrating disaster probabilities into the credit ratings model, further improves the ROC-AUC to 0.97 and the PR-AUC to 0.92. The exceptionally high performance of these models can be justified by the nature of defaults, which rarely occur as sudden surprises. Instead, they are often the result of prolonged processes and involve a self-fulfilling component as investor pessimism increases borrowing costs.

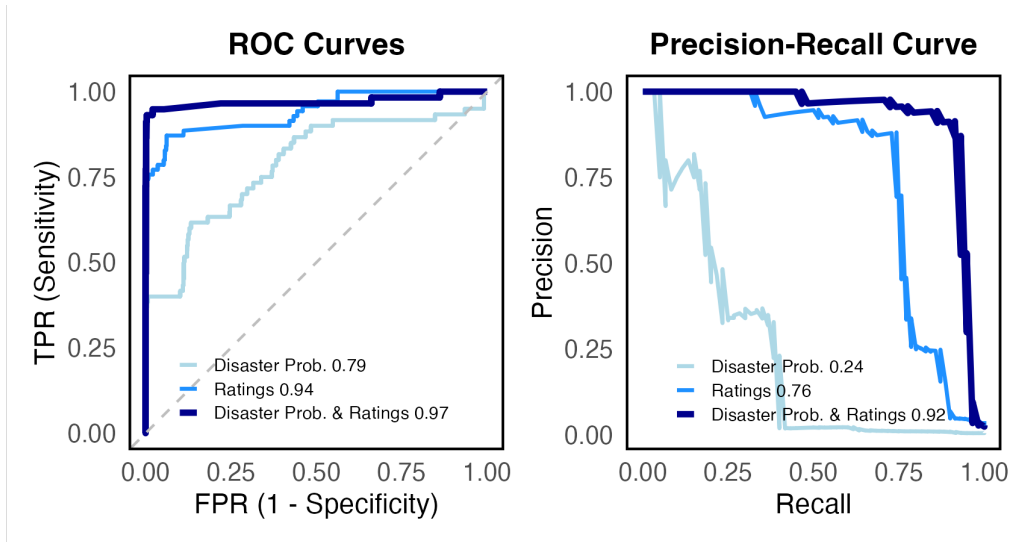


Figure 10: Predictive performance of disaster probabilities and credit ratings for disasters

Notes: The figure shows the predictive performance of three different models for forecasting disasters: using only disaster probabilities, using only credit rating variables (including the current rating, the magnitude of the last downgrade and upgrade, and the time since the last downgrade and upgrade), and using both sources. Disaster probabilities are used directly, while the other models rely on a Random Forest model. All models are implemented using an expanding window forecasting method.

Source: Author's calculations.

These results show that both approaches are better at predicting disasters than credit rating changes, as expected, given their purpose. Credit ratings remain the stronger standalone predictor with a very high performance. Yet, disaster probabilities improve the model further, highlighting the informational value of bond market data in forecasting events.

5 Conclusions

This paper introduces a novel approach to estimating investors' perceived probability of disaster from yield curve data. I provide daily estimates of the one-year-ahead disaster probability as perceived by investors for around 60 countries from 2000 to 2023. Then, I demonstrate the predictive value of these probabilities through several exercises.

Disaster probabilities spike before major events, such as debt restructurings in Greece, Sri Lanka, and Ghana, and the onset of the Russia-Ukraine war, with probabilities reaching 100% months in advance in some cases. These probabilities are positively correlated with credit ratings, remaining low for most ratings and increasing sharply for higher-risk ratings. Finally, the estimated probabilities enhance the predictive power of credit ratings for predicting future downgrades and disaster events.

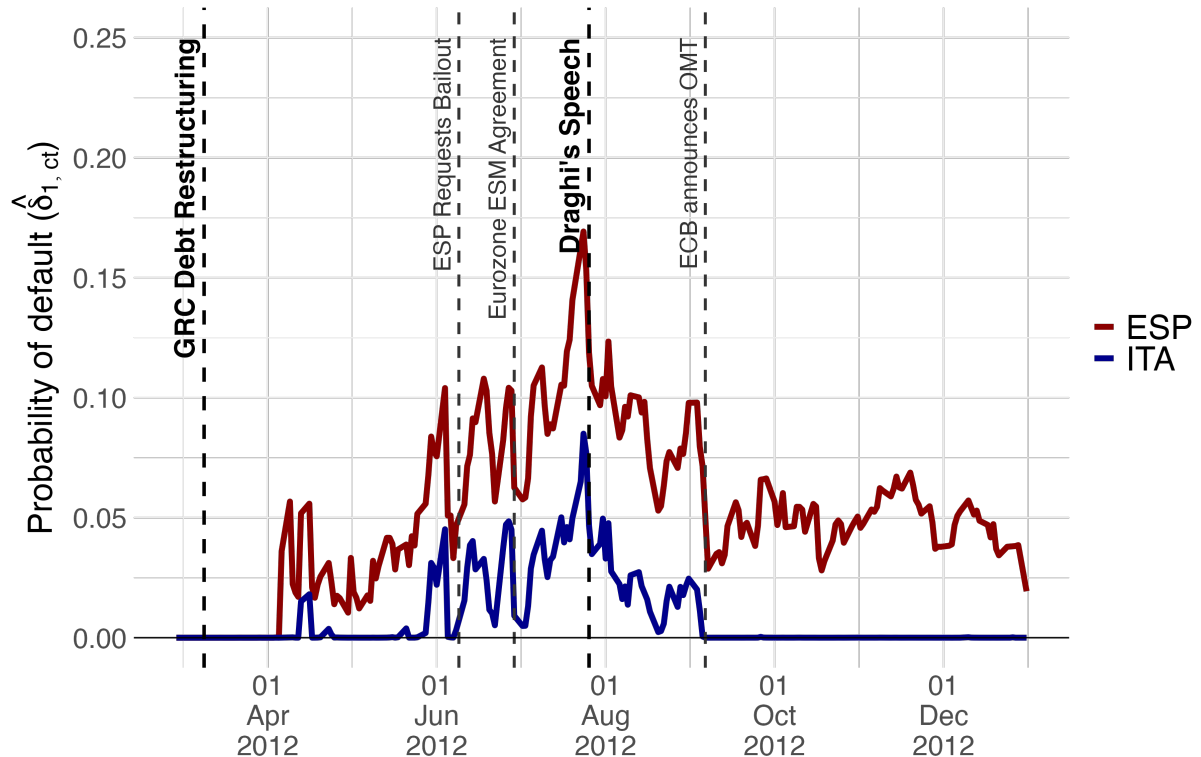


Figure 11: Evolution of probability of default for Spain and Italy

Notes: The figure shows the evolution of the probability of default for Spain and Italy. Vertical lines represent relevant events.

Source: Author's calculations.

The disaster probabilities estimated in this study have numerous potential applications that extend beyond their predictive capabilities. One compelling application is their use identifying effective policies for calming investor fears. Figure 11 shows the evolution of the estimated probability of default for Spain and Italy from Greece's debt restructuring in March 2012 to January 2013. Several policy measures were implemented to address the rising risk, including Spain's request for a bank bailout to recapitalize its financial institutions and the establishment of the European Stability Mechanism (ESM) to provide

financial assistance and stabilize the banking sector regionally. While these actions offered some short-term relief, it was Draghi’s declaration to “do whatever it takes to preserve the euro” that marked a sharp decline in perceived risk, effectively reversing the prior upward trend. Other potential applications include estimating the welfare implications of such policies or analyzing spillover effects from disasters.

Finally, future research can address the model’s limitations. First, there is room for improvement in the performance of the theoretical model. Expanding the model to incorporate additional instruments, such as equities and corporate bonds, and developing a general equilibrium framework could more accurately capture the data-generating process. This would improve theoretical price estimations and enhance the identification of disaster risk. Another issue is the inability to distinguish between the probability of a disaster and its effect, as the model relies on general assumptions about the magnitude of disaster-related jumps. Calibrating these jumps to be country-specific or dependent on other variables could address this limitation. Additionally, the current approach requires specifying the type of disaster based on the country’s context, limiting the model’s use for long-term analysis as these contexts are likely to change. Integrating an NLP model to analyze news reports and text data could help identify not only the type of disaster but also its severity, allowing for a more precise estimation of disaster risk probabilities.

References

- Ang, Andrew, Monika Piazzesi, and Min Wei. 2006. “What does the yield curve tell us about GDP growth?” *Journal of econometrics* 131 (1-2): 359–403.
- Arrow, Kenneth J, Robert Forsythe, Michael Gorham, Robert Hahn, Robin Hanson, John O Ledyard, Saul Levmore, Robert Litan, Paul Milgrom, Forrest D Nelson, et al. 2008. *The promise of prediction markets*, 5878.
- Backus, David, Mikhail Chernov, and Ian Martin. 2011. “Disasters implied by equity index options.” *The journal of finance* 66 (6): 1969–2012.
- Barro, Robert J. 2006. “Rare disasters and asset markets in the twentieth century.” *The Quarterly Journal of Economics* 121 (3): 823–866.
- Barro, Robert J, and Gordon Y Liao. 2021. “Rare disaster probability and options pricing.” *Journal of Financial Economics* 139 (3): 750–769.
- Bekaert, Geert, Campbell R Harvey, Christian T Lundblad, and Stephan Siegel. 2016. “Political risk and international valuation.” *Journal of Corporate Finance* 37:1–23.
- Berkman, Henk, Ben Jacobsen, and John B Lee. 2011. “Time-varying rare disaster risk and stock returns.” *Journal of Financial Economics* 101 (2): 313–332.

- Bharath, Sreedhar T, and Tyler Shumway. 2008. "Forecasting default with the Merton distance to default model." *The Review of Financial Studies* 21 (3): 1339–1369.
- Blinder, Alan S, Michael Ehrmann, Marcel Fratzscher, Jakob De Haan, and David-Jan Jansen. 2008. "Central bank communication and monetary policy: A survey of theory and evidence." *Journal of economic literature* 46 (4): 910–945.
- Bluwstein, Kristina, Marcus Buckmann, Andreas Joseph, Sujit Kapadia, and Özgür Şimşek. 2023. "Credit growth, the yield curve and financial crisis prediction: Evidence from a machine learning approach." *Journal of International Economics* 145:103773.
- Chadefaux, Thomas. 2017. "Market anticipations of conflict onsets." *Journal of Peace Research* 54 (2): 313–327.
- Clark, Ephraim. 1997. "Valuing political risk." *Journal of International Money and Finance* 16 (3): 477–490.
- Cochrane, John. 2009. *Asset pricing: Revised edition*. Princeton university press.
- De Grauwe, Paul, and Yuemei Ji. 2013. "Self-fulfilling crises in the Eurozone: An empirical test." *Journal of International Money and finance* 34:15–36.
- Dionne, Georges, Genevieve Gauthier, Khemais Hammami, Mathieu Maurice, and Jean-Guy Simonato. 2010. "Default risk in corporate yield spreads." *Financial Management* 39 (2): 707–731.
- Duffee, Gregory R. 1999. "Estimating the price of default risk." *The Review of financial studies* 12 (1): 197–226.
- Estrella, Arturo, and Gikas A Hardouvelis. 1991. "The term structure as a predictor of real economic activity." *The journal of Finance* 46 (2): 555–576.
- Estrella, Arturo, and Frederic S Mishkin. 1998. "Predicting US recessions: Financial variables as leading indicators." *Review of Economics and Statistics* 80 (1): 45–61.
- Fama, Eugene F. 1970. "Efficient capital markets." *Journal of finance* 25 (2): 383–417.
- Fang, Xiang, Bryan Hardy, and Karen K Lewis. 2022. *Who holds sovereign debt and why it matters*. Technical report. National Bureau of Economic Research.
- Farhi, Emmanuel, and Xavier Gabaix. 2016. "Rare disasters and exchange rates." *The Quarterly Journal of Economics* 131 (1): 1–52.
- Gabaix, Xavier. 2008. "Variable rare disasters: A tractable theory of ten puzzles in macro-finance." *American Economic Review* 98 (2): 64–67.

- Gabaix, Xavier. 2012. “Variable rare disasters: An exactly solved framework for ten puzzles in macro-finance.” *The Quarterly journal of economics* 127 (2): 645–700.
- Gilchrist, S, E Zakrjsek, G Favara, and K Lewis. 2016. “Recession risk and the excess bond premium.” *Fed Notes*, no. 8, 1–3.
- Gilchrist, Simon, and Egon Zakrajšek. 2012. “Credit spreads and business cycle fluctuations.” *American economic review* 102 (4): 1692–1720.
- Gourio, Francois. 2012. “Disaster risk and business cycles.” *American Economic Review* 102 (6): 2734–2766.
- Huang, Tao, Fei Wu, Jing Yu, and Bohui Zhang. 2015. “International political risk and government bond pricing.” *Journal of Banking & Finance* 55:393–405.
- Julliard, Christian, and Anisha Ghosh. 2012. “Can rare events explain the equity premium puzzle?” *The Review of Financial Studies* 25 (10): 3037–3076.
- Leippold, Markus, and Felix Matthys. 2022. “Economic policy uncertainty and the yield curve.” *Review of Finance* 26 (4): 751–797.
- Lorenzoni, Guido, and Ivan Werning. 2019. “Slow moving debt crises.” *American Economic Review* 109 (9): 3229–3263.
- Luckner, Clemens Graf von, Josefin Meyer, Carmen M Reinhart, and Christoph Trebesch. 2023. “Sovereign Debt: 200 years of creditor losses.”
- Malkiel, Burton G. 2003. “The efficient market hypothesis and its critics.” *Journal of economic perspectives* 17 (1): 59–82.
- Merton, Robert C. 1974. “On the pricing of corporate debt: The risk structure of interest rates.” *The Journal of finance* 29 (2): 449–470.
- Meyer, Josefin, Carmen M Reinhart, and Christoph Trebesch. 2022. “Sovereign bonds since Waterloo.” *The Quarterly Journal of Economics* 137 (3): 1615–1680.
- Pástor, L'uboš, and Pietro Veronesi. 2013. “Political uncertainty and risk premia.” *Journal of financial Economics* 110 (3): 520–545.
- Reinhart, Carmen M, and Kenneth S Rogoff. 2010. “Growth in a Time of Debt.” *American economic review* 100 (2): 573–578.
- Remolona, Eli M, Michela Scatigna, and Eliza Wu. 2007. “Interpreting sovereign spreads.” *BIS Quarterly Review, March*.

- Rietz, Thomas A. 1988. “The equity risk premium a solution.” *Journal of monetary Economics* 22 (1): 117–131.
- Ross, Steve. 2015. “The recovery theorem.” *The Journal of Finance* 70 (2): 615–648.
- Rossi, Luca, Nick W. Kraemer, and Vaishali Singh. 2023. *Default, Transition, and Recovery: 2023 Annual Global Sovereign Default And Rating Transition Study*. Technical report. Six sovereigns defaulted in 2023, reflecting challenges in emerging and frontier markets. S&P Global Ratings Credit Research & Insights. <https://www.spglobal.com/ratings/en/research-insights>.
- Schreindorfer, David. 2020. “Macroeconomic tail risks and asset prices.” *The Review of Financial Studies* 33 (8): 3541–3582.
- Smales, Lee A. 2016. “The role of political uncertainty in Australian financial markets.” *Accounting & Finance* 56 (2): 545–575.
- Wachter, Jessica A. 2013. “Can time-varying risk of rare disasters explain aggregate stock market volatility?” *The Journal of Finance* 68 (3): 987–1035.
- Wolfers, Justin, and Eric Zitzewitz. 2004. “Prediction markets.” *Journal of economic perspectives* 18 (2): 107–126.

Appendices

A Derivations and proofs

A.1 Derivation of the price equation

For the 1-periods bond, the price is given by

$$\begin{aligned}
Q_{1t} &= \beta \mathbb{E}_t \left[\frac{F_{1t}}{G_{t+1}^\theta \Pi_{t+1}} \right] = \beta \mathbb{E}_t \left[\frac{Z_{t+1}}{(\alpha_G G_t^{\phi_G} \varepsilon_{t+1} V_{t+1})^\theta \alpha_\Pi \Pi_t^{\phi_\Pi} \eta_{t+1} W_{t+1}} \right] \\
&= \beta \frac{1}{(\alpha_G G_t^{\phi_G})^\theta \alpha_\Pi \Pi_t^{\phi_\Pi}} \mathbb{E}_t \left[\frac{1}{\varepsilon_{t+1}^\theta} \right] \mathbb{E}_t \left[\frac{1}{\eta_{t+1}} \right] \mathbb{E}_t \left[\frac{1}{V_{t+1}^\theta W_{t+1}} \right] \\
&= \beta \frac{1}{(\alpha_G G_t^{\phi_G})^\theta \alpha_\Pi \Pi_t^{\phi_\Pi}} \mathbb{E}_t \left[e^{-\log(\theta \varepsilon_{t+1})} \right] \mathbb{E}_t \left[e^{-\log(\eta_{t+1})} \right] \left(1 - \delta_{1,t} + \delta_{1,t} \frac{1 - \gamma J_F}{J_G^\theta J_\Pi} \right) \\
&= \beta \frac{e^{\frac{1}{2}((\theta \sigma_\varepsilon)^2 + \sigma_\eta^2)}}{(\alpha_G G_t^{\phi_G})^\theta \alpha_\Pi \Pi_t^{\phi_\Pi}} \left(1 + \delta_{1,t} \left(\frac{1 - \gamma J_F}{J_G^\theta J_\Pi} - 1 \right) \right)
\end{aligned} \tag{A1}$$

For the 2-periods bond, the price is given by

$$\begin{aligned}
Q_{2t} &= \beta^2 \mathbb{E}_t \left[\frac{1}{G_{t+1}^\theta G_{t+2}^\theta \Pi_{t+1} \Pi_{t+2}} \right] \\
&= \beta^2 \mathbb{E}_t \left[\frac{1}{G_{t+1}^\theta (\alpha_G G_{t+1}^{\phi_G} \varepsilon_{t+2} V_{t+2})^\theta \Pi_{t+1} (\alpha_\Pi \Pi_{t+1}^{\phi_\Pi} \eta_{t+2} W_{t+2})} \right] \\
&= \beta^2 \frac{1}{(\alpha_G^{2+\phi_G} G_t^{\phi_G + \phi_G^2})^\theta \alpha_\Pi^{2+\phi_\Pi} \Pi_t^{\phi_\Pi + \phi_\Pi^2}} \mathbb{E}_t \left[\frac{1}{\varepsilon_{t+1}^{(1+\phi_G)\theta}} \right] \mathbb{E}_t \left[\frac{1}{\varepsilon_{t+2}^\theta} \right] \mathbb{E}_t \left[\frac{1}{\eta_{t+1}^{1+\phi_\Pi}} \right] \mathbb{E}_t \left[\frac{1}{\eta_{t+2}} \right] \\
&\quad \mathbb{E}_t \left[\frac{Z_{t+1}}{V_{t+1}^\theta W_{t+1}} \right] \mathbb{E}_t \left[\frac{Z_{t+2}}{V_{t+2}^\theta W_{t+2}} \right] \\
&= \beta^2 \frac{e^{\frac{1}{2}((1+(1+\phi_G)^2)\theta^2 \sigma_\varepsilon^2 + (1+(1+\phi_\Pi)^2)\sigma_\eta^2)}}{(\alpha_G^{2+\phi_G} G_t^{\phi_G + \phi_G^2})^\theta \alpha_\Pi^{2+\phi_\Pi} \Pi_t^{\phi_\Pi + \phi_\Pi^2}} \left(1 + \delta_{1,t} \left(\frac{1 - \gamma J_F}{J_G^{(1+\phi_G)\theta} J_\Pi^{1+\phi_\Pi}} - 1 \right) \right) \left(1 + \delta_{2,t} \left(\frac{1 - \gamma J_F}{J_G^\theta J_\Pi} - 1 \right) \right)
\end{aligned} \tag{A2}$$

For the 3-periods bond, the price is given by

$$\begin{aligned}
Q_{3t} &= \beta^3 \frac{e^{\frac{1}{2}((1+(1+\phi_G)^2 + (1+\phi_G + \phi_G^2)^2)\theta^2 \sigma_\varepsilon^2 + (1+(1+\phi_\Pi)^2 + (1+\phi_\Pi + \phi_\Pi^2)^2)\sigma_\eta^2)}}{(\alpha_G^{3+2\phi_G+\phi_G^2} G_t^{\phi_G + \phi_G^2 + \phi_G^3})^\theta \alpha_\Pi^{3+2\phi_\Pi+\phi_\Pi^2} \Pi_t^{\phi_\Pi + \phi_\Pi^2 + \phi_\Pi^3}} \left(1 + \delta_{1,t} \left(\frac{1 - \gamma J_F}{J_G^{(1+\phi_G+\phi_G^2)\theta} J_\Pi^{1+\phi_\Pi+\phi_\Pi^2}} - 1 \right) \right) \\
&\quad \left(1 + \delta_{2,t} \left(\frac{1 - \gamma J_F}{J_G^{(1+\phi_G)\theta} J_\Pi^{1+\phi_\Pi}} - 1 \right) \right) \left(1 + \delta_{3,t} \left(\frac{1 - \gamma J_F}{J_G^\theta J_\Pi} - 1 \right) \right)
\end{aligned} \tag{A3}$$

Then, for the N-period bond,

$$Q_{Nt} = \beta^N \frac{e^{\frac{1}{2}(\sum_{i=1}^N (\sum_{j=0}^{i-1} \phi_G^j)^2 \theta^2 \sigma_\varepsilon^2 + \sum_{i=1}^N (\sum_{j=0}^{i-1} \phi_\Pi^j)^2 \sigma_\eta^2)}}{\left(\alpha_G^{\sum_{i=1}^N i \phi_G^{N-i}} G_t^{\sum_{i=1}^N \phi_G^i} \right)^\theta \alpha_\Pi^{\sum_{i=1}^N i \phi_\Pi^{N-i}} \Pi_t^{\sum_{i=1}^N \phi_\Pi^i}} \prod_{\tau=1}^N \left(1 + \delta_{\tau,t} \left(\frac{1}{J_G^{\sum_{j=1}^{N+1-i} \theta \phi_G^{j-1}} J_\Pi^{\sum_{j=1}^{N+1-i} \phi_\Pi^{j-1}}} - 1 \right) \right)} \quad (\text{A4})$$

A.2 Proof of Proposition 1

I use the logarithmic differentiation trick. Taking the logarithm of Equation 14:

$$\log(Q_{Nt}) = \log(Q^{ND}) + \sum_{\tau=1}^N \log \left(1 + \phi_\delta^{\tau-1} \delta_{1,t} (J_{\tau,N} - 1) \right) \quad (\text{A5})$$

Then, differentiating with respect to $\delta_{1,t}$,

$$\begin{aligned} \frac{\partial \log(Q_{Nt})}{\partial \delta_{1,t}} &= \sum_{\tau=1}^N \frac{\phi_\delta^{\tau-1} (J_{\tau,cN} - 1)}{1 + \phi_\delta^{\tau-1} \delta_{1,t} (J_{\tau,N} - 1)} \\ \frac{1}{Q_{Nt}} \frac{\partial Q_{Nt}}{\partial \delta_{1,t}} &= \sum_{\tau=1}^N \frac{\phi_\delta^{\tau-1} (J_{\tau,cN} - 1)}{1 + \phi_\delta^{\tau-1} \delta_{1,t} (J_{\tau,N} - 1)} \\ \frac{\partial Q_{Nt}}{\partial \delta_{1,t}} &= Q_{Nt} \sum_{\tau=1}^N \frac{\phi_\delta^{\tau-1} (J_{\tau,cN} - 1)}{1 + \phi_\delta^{\tau-1} \delta_{1,t} (J_{\tau,N} - 1)} \end{aligned} \quad (\text{A6})$$

Since $Q_{Nt} > 0$, the sign of $\frac{\partial Q_{Nt}}{\partial \delta_{1,t}}$ is determined by the sign of the second element, which proves the first part of the proposition.

Because the denominator in each term is always positive ($1 + \phi_\delta^{\tau-1} \delta_{1,t} (J_{\tau,N} - 1) > 0$ and $\phi_\delta > 0$), the sign of each element in the sum depends on the sign of $J_{\tau,N} - 1$. The sum includes all periods until maturity, with each term weighted by a positive denominator. Therefore, if all $J_{\tau,N} < 1$, then each term in the sum is negative, and thus the price decreases with an increase in $\delta_{1,t}$.

B Appendix Figures

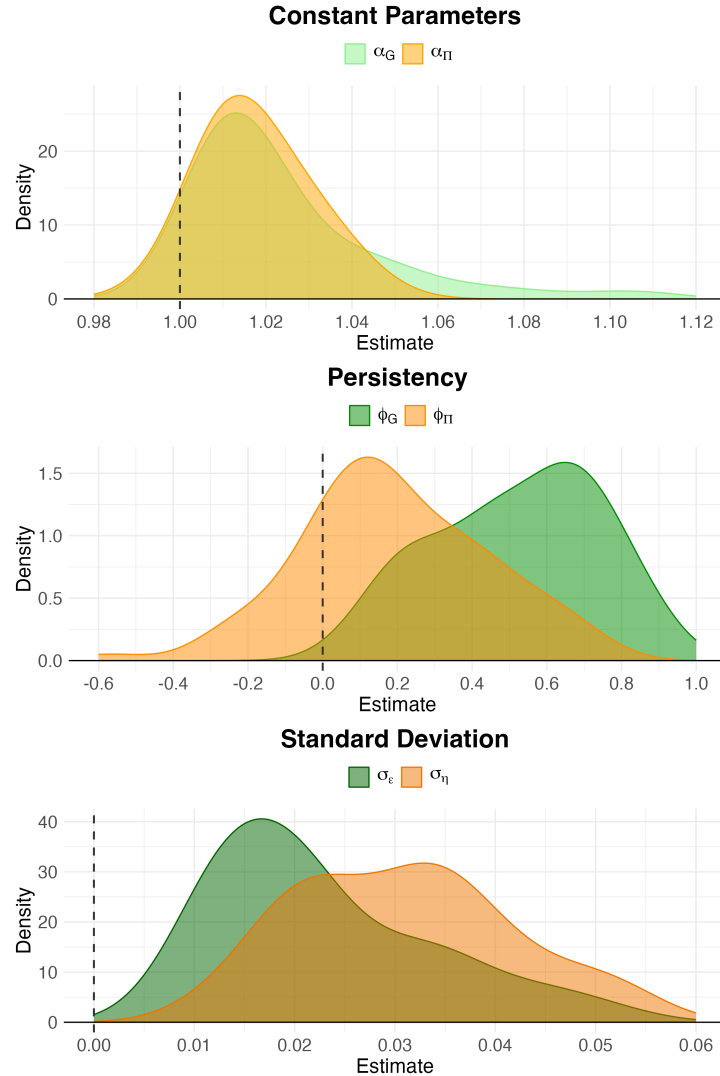


Figure B1: Distribution of estimates from laws of motion

Notes: The figure shows the kernel density of the estimates for α_G , α_Π , ϕ_G , ϕ_Π , σ_ε , and σ_η . The density plots for the constant parameters use a bandwidth of 0.01, for the persistency parameters a bandwidth of 0.1, and for the residual standard deviations a bandwidth of 0.005.

Source: Author's calculations.

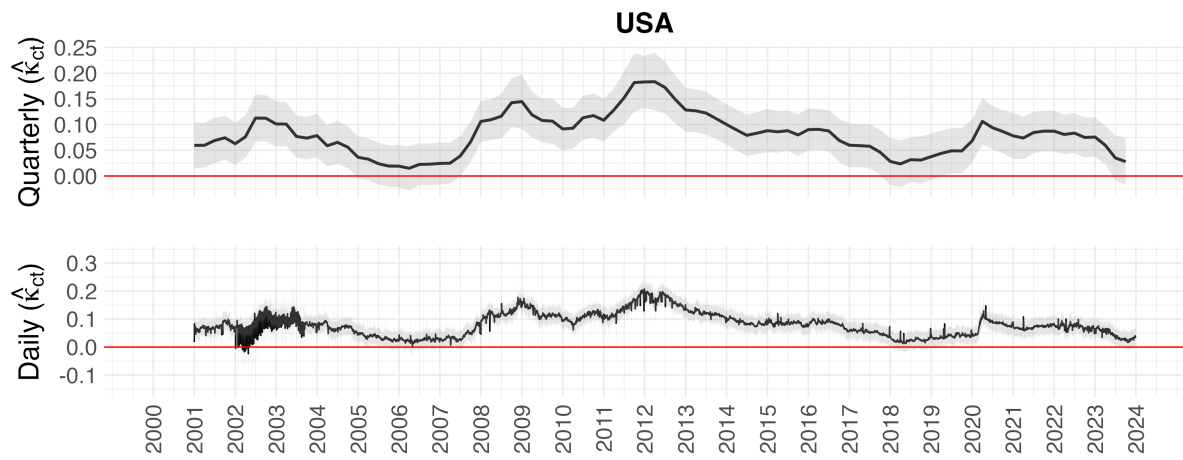


Figure B2: Comparison between daily and quarterly model

Notes: The figure shows the evolution of $\hat{\kappa}_{ct}$ with 95% confidence intervals for the US using daily and quarterly data. The line at 0 represents a reference threshold.

Source: Author's calculations.

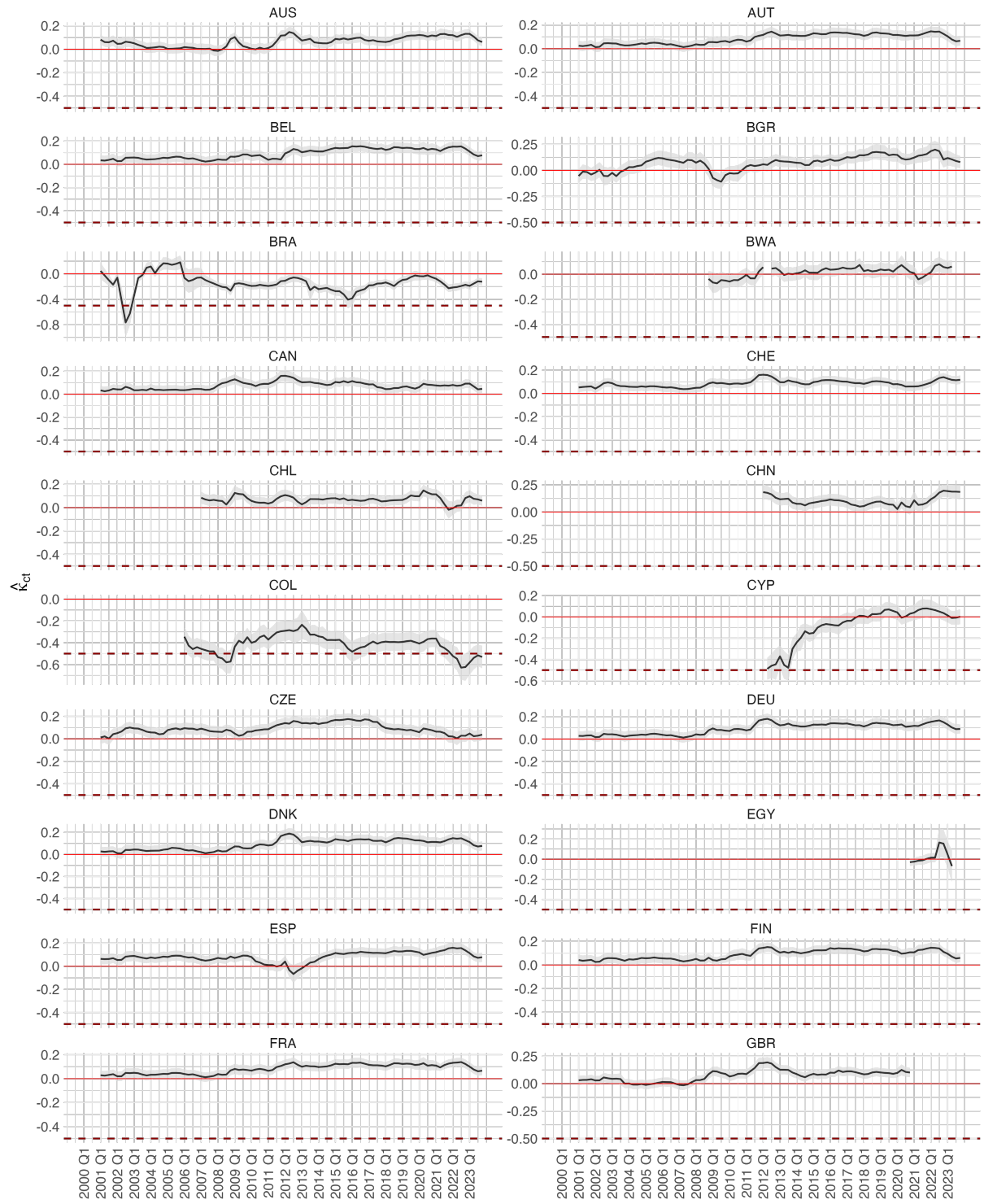


Figure B3: $\hat{\kappa}_{ct}$ for all countries - part 1

Notes: The figure shows the evolution of $\hat{\kappa}_{ct}$ with 95% confidence intervals. The lines at 0 and -0.5 represent reference thresholds. The values are estimated based on the quarterly model.

Source: Author's calculations.

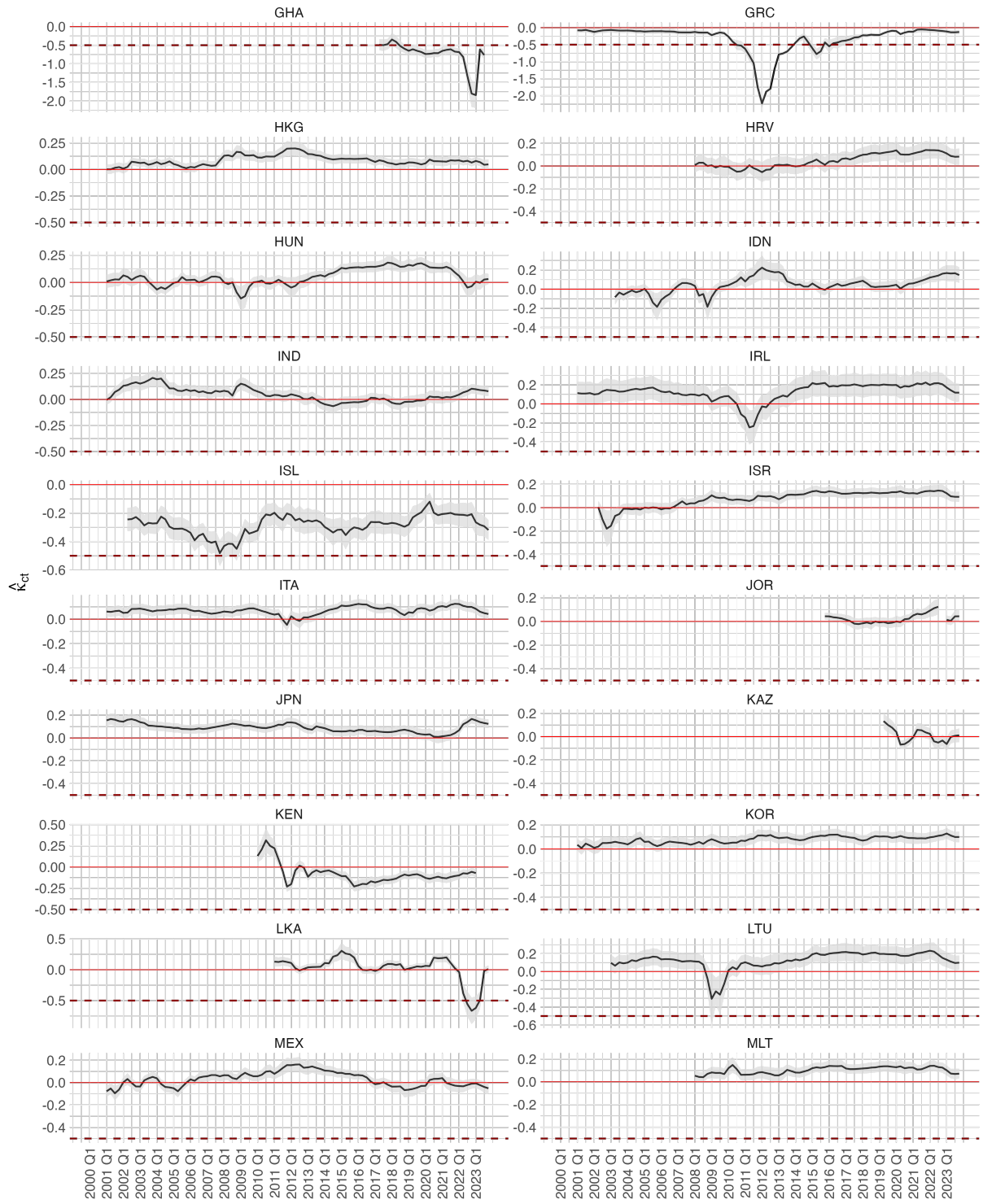


Figure B4: $\hat{\kappa}_{ct}$ for all countries - part 2

Notes: The figure shows the evolution of $\hat{\kappa}_{ct}$ with 95% confidence intervals. The lines at 0 and -0.5 represent reference thresholds. The values are estimated based on the quarterly model.

Source: Author's calculations.

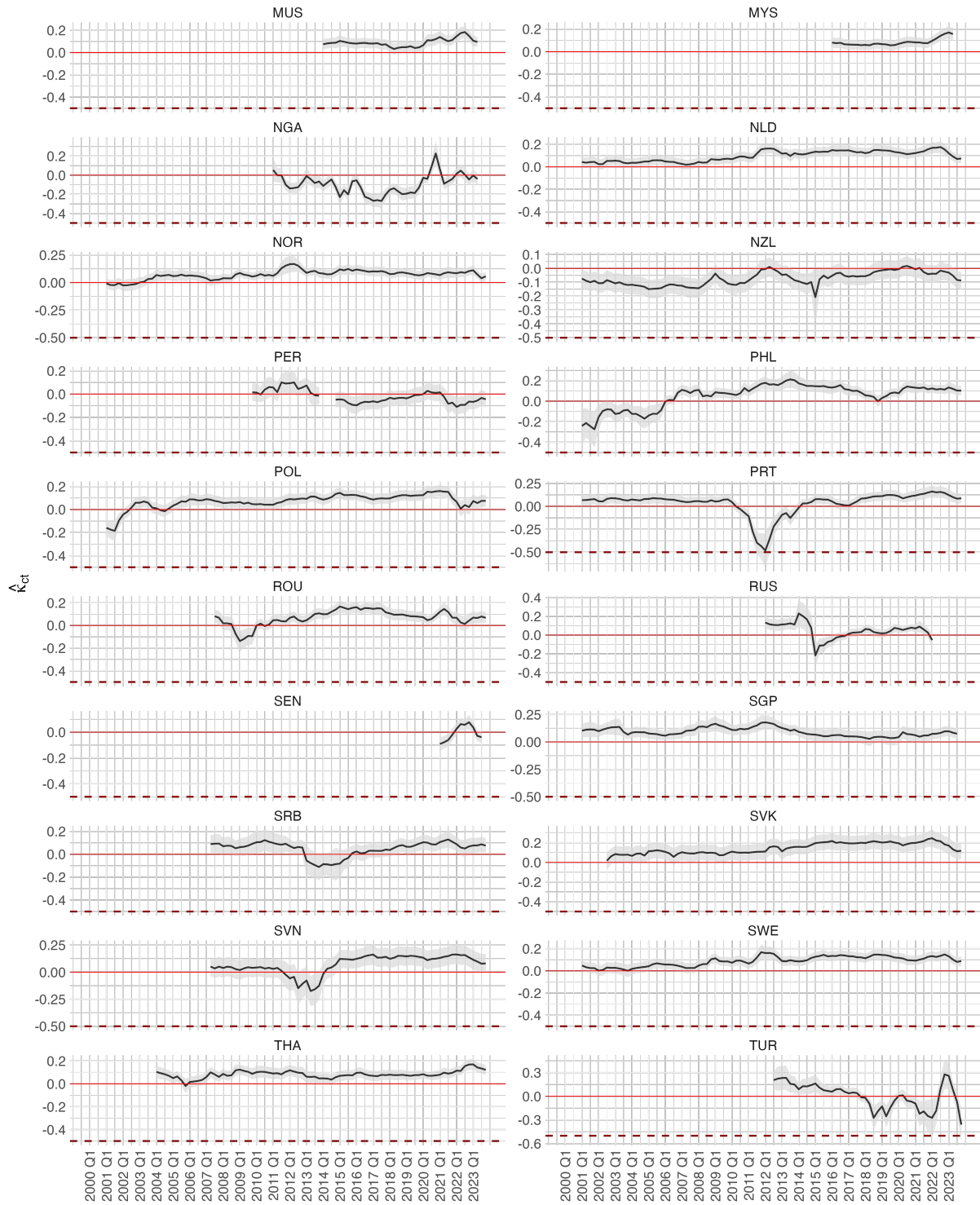


Figure B5: $\hat{\kappa}_{ct}$ for all countries - part 3

Notes: The figure shows the evolution of $\hat{\kappa}_{ct}$ with 95% confidence intervals. The red line at 0 represents reference thresholds.

The values are estimated based on the quarterly model.

Source: Author's calculations.

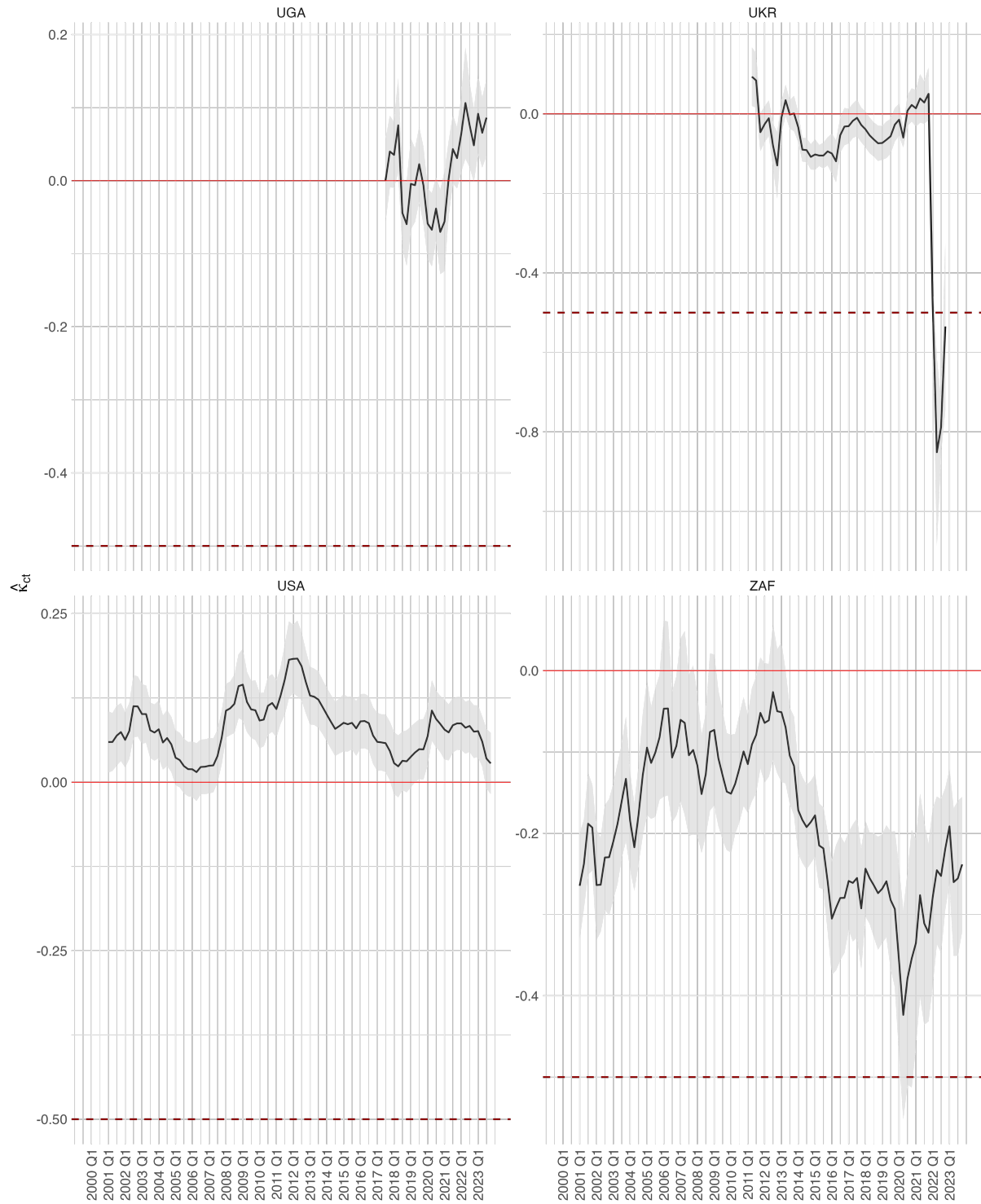


Figure B6: $\hat{\kappa}_{ct}$ for all countries - part 4

Notes: The figure shows the evolution of $\hat{\kappa}_{ct}$ with 95% confidence intervals. The lines at 0 and -0.5 represent reference thresholds. The values are estimated based on the quarterly model.

Source: Author's calculations.

C Appendix Tables

Table C1: Yield curve data overview: country coverage, time span, and maturities

Isocode	Start date	End date	Maturities	Isocode	Start date	End date	Maturities
AUS	2001-01-01	2023-12-29	1-10	AUT	2001-01-01	2023-12-29	1-10
BEL	2001-01-02	2023-12-29	2-10	BGR	2001-02-19	2023-12-29	1-5, 7, 10
BRA	2001-01-05	2023-12-28	1-3, 5, 8, 10	BWA	2008-10-27	2023-06-02	3
CAN	2001-01-02	2023-12-29	1-5, 7, 10	CHE	2001-01-02	2023-12-29	1-10
CHL	2007-03-26	2023-12-29	1, 2, 4, 5, 8, 10	CHN	2012-01-04	2023-12-29	1-3, 5, 7, 10
COL	2006-01-02	2023-12-29	2, 4, 5, 10	CYP	2012-04-27	2023-12-29	2-4, 7, 10
CZE	2001-01-02	2023-12-29	1-10	DEU	2001-01-01	2023-12-29	1-10
DNK	2001-01-02	2023-12-29	2, 3, 5, 8, 10	EGY	2020-10-01	2023-06-30	1-3, 5, 7, 10
ESP	2001-01-02	2023-12-29	1-10	FIN	2001-01-02	2023-12-29	2-6, 8, 10
FRA	2001-01-01	2023-12-29	1-10	GBR	2001-01-01	2020-12-31	1-10
GHA	2017-04-20	2023-09-29	4, 5, 7, 8, 10	GRC	2001-01-03	2023-12-29	1-3, 5, 7, 10
HKG	2001-01-02	2023-12-29	1-3, 5, 7, 10	HRV	2008-01-30	2023-12-29	1-5, 10
HUN	2001-01-02	2023-12-29	1, 3, 5, 10	IDN	2003-05-14	2023-12-29	1, 3, 5, 10
IND	2001-01-01	2023-12-29	1-10	IRL	2001-01-02	2023-12-29	1-10
ISL	2002-04-15	2023-12-29	2, 5, 10	ISR	2002-04-09	2023-12-28	1-3, 5, 10
ITA	2001-01-02	2023-12-29	1-10	JOR	2015-10-06	2023-12-28	1-3, 5, 7, 10
JPN	2001-01-04	2023-12-29	1-10	KAZ	2019-04-19	2023-12-29	1-10
KEN	2010-01-04	2023-03-31	1-10	KOR	2001-01-02	2023-12-29	1-5, 10
LKA	2011-01-03	2023-12-29	1-10	LTU	2003-01-20	2023-12-29	3, 5, 10
MEX	2001-01-02	2023-12-29	1, 3, 5, 7, 10	MLT	2008-02-29	2023-12-29	1, 3, 5, 10
MUS	2014-01-22	2023-06-30	1-5, 10	MYS	2016-01-04	2023-06-30	1, 3, 5, 7, 10
NGA	2011-01-04	2023-06-30	1-5, 7, 10	NLD	2001-01-01	2023-12-29	2-10
NOR	2001-01-01	2023-12-29	1, 3, 5, 10	NZL	2001-01-03	2023-12-29	1, 2, 5, 7, 10
PER	2009-10-28	2023-12-29	2, 5, 10	PHL	2001-01-02	2023-12-29	1-5, 7, 10
POL	2001-01-02	2023-12-29	1-8, 10	PRT	2001-01-01	2023-12-29	1-10
ROU	2007-08-16	2023-12-29	1-5, 7, 10	RUS	2012-01-04	2022-03-31	1-3, 5, 7, 10
SEN	2021-03-24	2023-09-29	3, 5, 7	SGP	2001-01-02	2023-09-29	1, 2, 5, 10
SRB	2007-05-04	2023-12-28	1-3, 5, 10	SVK	2002-07-26	2023-12-29	2, 5, 6, 8-10
SVN	2007-04-03	2023-12-29	1, 3-5, 7, 8, 10	SWE	2001-01-02	2023-12-29	2, 5, 7, 10
THA	2004-01-05	2023-12-28	1-5, 7, 10	TUR	2012-07-02	2023-12-29	1-3, 5, 10
UGA	2017-07-03	2023-09-29	1-3, 5, 10	UKR	2011-04-01	2022-12-30	1-3, 6
USA	2001-01-01	2023-12-29	1-3, 5, 7, 10	ZAF	2001-01-02	2023-12-29	5, 10

Notes: This table provides an overview of yield curve data for 64 countries, showing the respective time spans and bond maturities between 1 and 10 years used in the analysis. The data is based on benchmark bonds.

Source: Datastream.

Table C2: Fixed effects regression: impact of war on consumption growth and inflation

	Growth _t (1)	Inflation _t (2)
War _t	-0.023*** (0.004)	0.018*** (0.004)
Growth _{t-1}	0.164*** (0.014)	
Inflation _{t-1}		0.526***
Country FE	✓	✓
Time FE	✓	✓
Observations	5,730	5,242
Adjusted R ²	0.003	0.290

Note: This table presents fixed effects regressions examining the impact of war on consumption growth (Growth_t) and inflation (Inflation_t). The regression equations are: $\log(\text{Growth}_t) = \beta_1^G \text{War}_t + \beta_2^G \log(\text{Growth}_{t-1}) + \kappa_c + \kappa_t + \epsilon_{it}$, $\log(\text{Inflation}_t) = \beta_1^{\Pi} \text{War}_t + \beta_2^{\Pi} \log(\text{Inflation}_{t-1}) + \kappa_c + \kappa_t + \epsilon_{it}$. Robust standard errors are reported in parentheses, with * $p < 0.1$, ** $p < 0.05$, and *** $p < 0.01$ indicating significance levels.

Source: WB/WDI and UCDP/GED data.

Table C3: Fixed effect regression: quarterly model

	Observed price (q_{Nct})				
	(1)	(2)	(3)	(4)	(5)
Non-disaster price (\hat{q}_{Nct}^{ND})	0.108*** (0.008)	0.206*** (0.010)	0.213*** (0.003)	0.316*** (0.001)	0.294*** (0.001)
Country-time FE	✓	✓	✓	✓	
Maturity-country FE	✓	✓			
Maturity-time FE	✓		✓		
Observations	28,725	28,725	28,725	28,725	28,725
Adjusted R ²	0.973	0.947	0.846	0.828	0.351

Note: This table presents a fixed effects regression of the observed log bond price ($q_{Nct} = \log(Q_{Nct})$) on the log of the theoretical non-disaster price ($q_{Nct}^{ND} = \log(Q_{Nct}^{ND})$). Fixed effects are denoted as κ_{Nc} (Maturity-Country), κ_{Nt} (Maturity-Time), and κ_{ct} (Country-Time). Models differ by their inclusion of these fixed effects. Robust standard errors are reported in parentheses, with * $p < 0.1$, ** $p < 0.05$, and *** $p < 0.01$ indicating significance levels.

Source: Author's calculations using Datastream data for observed prices.